# HEAT TRANSFER MEASUREMENTS IN FILM CONDENSATION OF STEAM ON SMALL DIAMETER HORIZONTAL TUBES

by

Mazhar Ünsal

Thesis submitted to the Graduate Faculty of the
Virginia Polytechnic Institute and State University
in partial fulfillment of the requirements for the degree of

MASTER OF SCIENCE

in

Mechanical Engineering

APPROVED:

William C. Thomas, Chairman

Robert A. Comparin

Walter F. O'Brien

April, 1972

Blacksburg, Virginia

## ACKNOWLEDGMENTS

The author wishes to express thanks and appreciation to his major professor, Dr. William C. Thomas for his encouragement and guidance during the research and preparation of this thesis. The author wishes to extend thanks to his advisory committee members.

The author also wants to acknowledge the Mechanical Engineering Department of Virginia Polytechnic Institute and State University for providing financial support by way of a Graduate Teaching Assistantship.

TABLE OF CONTENTS

## LIST OF TABLES

## LIST OF FIGURES

LIST OF FIGURES - continued

## NOMENCLATURE

| | |
|---|---|
| a | Y-intercept in Wilson's plot |
| A | area |
| b | slope in Wilson's plot |
| c | specific heat capacity |
| D | diameter |
| g | gravitational constant |
| h | heat transfer coefficient |
| k | thermal conductivity |
| L | length of test section |
| m | mass flow rate |
| $N_d$ | dimensionless number, $8\sigma/\pi\rho g D_o^2$ |
| $N_{Oh}$ | Ohnesorge number, $\mu/[\rho g D \sigma]^{1/2}$ |
| Nu | Nusselt number, hD/k |
| P | pressure |
| Pr | Prandtl number, $c\mu/k$ |
| q | total heat transfer |
| $q''_w$ | wall heat flux |
| r | radius of curvature |
| R | thermal resistance |
| Re | Reynolds number, $4m/\pi\mu D_i$ |
| T | temperature |
| $\Delta T$ | mean temperature difference |
| U | overall heat transfer coefficient |

| | |
|---|---|
| $V$ | mean velocity |
| $X$ | abscissa in Wilson's plot, $[1/V]^{0.83}$ |
| $y$ | coordinate measuring distance normal to tube wall |
| $Y$ | ordinate in Wilson's plot, $1/UA$ |
| $\rho$ | density |
| $\mu$ | viscosity |
| $\lambda$ | latent heat of vaporization |
| $\sigma$ | surface tension |
| $\delta$ | average thickness of the condensate film |
| $\xi$ | acceleration effect parameter, $k(T_{f,a})[T_{s,a}-T_{w,o,a}]/\mu(T_{f,a})\lambda(T_{s,a})$ |
| $\zeta$ | heat capacity parameter, $c[T_{s,a}-T_{w,o,a}]/\lambda(T_{s,a})$ |

Subscripts

| | |
|---|---|
| a | average |
| c | calculated using analytical solution |
| f | pertaining to condensate film |
| i | pertaining to inside of tube |
| m | measured |
| Nu | calculated using Nusselt's equation |
| o | pertaining to outside of tube |
| s | pertaining to steam |
| t | total |
| w | pertaining to tube wall |
| v | pertaining to vapor |

| | |
|---|---|
| 1 | pertaining to test section inlet |
| 2 | pertaining to test section exit |

# I. INTRODUCTION

Heat transfer during vapor condensation is a common problem in many industrial processes and has been studied by hundreds of investigators. Initial research on condensation, which started early in the twentieth century, was motivated by attempts to improve heat exchanger design. Many of the experimental studies of condensation heat transfer have been conducted using horizontal tubes as the condensing surface. The condenser tubes used in all the reported investigations had diameters larger than 0.6 inches. The present experimental study is concerned with condensation heat transfer on small diameter horizontal tubes. It is shown that the heat transfer rates are affected by surface tension for the small tube diameters.

## Background

When a vapor comes in contact with a solid surface which is below the saturation temperature of the vapor, condensation of the vapor to its liquid phase takes place in the vicinity of the solid surface. The thickness of the condensate tends to increase as more vapor condenses and collects on the surface until an equilibrium thickness is reached as determined by the mechanics of the specific physical system. The condensate buildup on the surface becomes an added resistance to heat transfer from the vapor-liquid interface to the solid surface. If the condensate completely wets the surface, it appears as a uniform liquid film over the surface. This condition is called film condensation. If the condensate does not completely wet the surface, it appears in

the form of attached drops streaks of films with differing thicknesses, or in a mixed condensation mode where different patterns exist adjacent to each other on the condensing surface.

Fluid mechanics and heat transfer theory for film condensation have been used successfully to predict heat transfer rates for a wide range of applications. Theories of dropwise condensation are, at the present time, insufficiently established to be useful in predicting heat transfer rates in dropwise condensation [1]. The prediction of the condensation mode for a vapor on a surface of a given texture is a problem that must be considered simultaneously with heat transfer analysis since a knowledge of the condensation mode is also necessary for accurately predicting the heat transfer rate. The interfacial tensions between the vapor, condensate and condensing surface are generally believed to determine the condensation pattern on the condensing surface [2].

## Effects of Scale Formation and Condensation Type in Heat Transfer Measurements

Condensation heat transfer measurements with industrial heat exchangers have shown that scale formation on the heat exchanger surfaces reduces the amount of heat transferred. Scale is defined as any kind of deposit layer which forms after prolonged use of the heat exchanger apparatus. The major constituent of scale is silicon oxide which has a low thermal conductivity so that small amounts of deposit result in a large reduction in the heat transfer rate. Added resistance to heat transfer resulting from scaling has been determined by comparing old

and new measurements for tube-type condensers [3]. Heat transfer coefficients which account for scale deposits in different systems are listed in reference 4. If a scale deposit is present in heat transfer measuring equipment, it is necessary to know the precise value of the thermal resistance of the deposit layer in order to deduce the heat transfer coefficient of the condensate layer from the experimental results. A direct measurement of the scale thermal resistance, however, has not been reported in the literature.

Condensation type or pattern has a significant effect on heat transfer rates. The heat transfer coefficients reported for dropwise or mixed modes are severalfold larger than those reported for film condensation. On the basis of experiments by many investigators, Jakob [5] concluded that clean steam always condenses as a film on clean surfaces whether rough or polished and that dropwise condensation of steam does not occur unless the cooling surface is contaminated in some way. Hampson [6,7] studied condensation modes on vertical flat plates. According to his experimental results for different surface preparation procedures, a completely dropwise mode of condensation can be obtained only on a carefully prepared (contaminated) surface. The following quote from reference 7 summarizes the investigator's findings:

> "Any contaminant in the vapour will eventually affect the mode of condensation. This usual mode is one which is intermediate between dropwise and filmwise, and is described as 'mixed' condensation. In practice, the purely dropwise or filmwise modes of condensation are usually found to be transitory ones, and the customary mode is one of 'mixed' condensation during which small irregular areas of liquid, resembling flattened drops, are separated by narrow lanes which appear to be free of liquid."

Condensation Heat Transfer on Horizontal Tubes

The first mathematical solution for laminar film condensation on a horizontal tube was given by Nusselt in 1916 [8]. Nusselt considered the gravity and viscous forces only. Assuming a two-dimensional flow pattern and a linear temperature profile across the condensate film, he used the mass, momentum, and energy conservation equations to find the following expression for the heat transfer coefficient

$$h_{Nu} = 0.725\ [\lambda\rho^2 g k^3/\mu D(T_v - T_w)]^{1/4} \cdot$$

The heat transfer coefficients calculated by this expression were then compared to experimentally measured values. The ratio of measured to calculated heat transfer coefficients from experimental results of different investigators are presented in references 4, 9, and 10. The measured coefficients show a large difference from Nusselt's solution, i.e.,

$$0.6 < h/h_{Nu} < 2.4$$

It is important to note, however, that most of the above experimental measurements were carried out under conditions which did not permit direct visual observation of the flow pattern [9,11,12,13,14]. The results of some of the experimental arrangements where the vapor flows with respect to the condensing surface may include additional deviations resulting from the non-negligible shear stress at the condensate-vapor interface. Baker and Mueller [15] observed film condensation when condensing pure vapors of benzene and of water. A comparison with

Nusselt's equation was not given by them.

Some experimenters [14,16] emphasize the importance of tube standardization before starting experimental measurements in order to obtain consistency and repeatability between measured coefficients. The standardization procedure consists of letting the experimental system remain in operation for a period of time before starting measurements. Henderson [16] presents the following observation:

> "After the apparatus had been in use for several months, it was noted that the condensate film had become more continuous. It was also noted that the experimental heat transfer coefficients had become more predictable. The data obtained during the earliest runs had much higher heat transfer coefficients than those obtained later. This was assumed to be caused by the formation of a thin deposit layer on the tube. All of the data taken before the deposit formation was completed were discarded."

The overall heat transfer resistance measured in Henderson's experimental study included the film resistance and the scale resistance. The experimental system was not designed for a direct measurement of the scale resistance. Henderson assumed the validity of Nusselt's equation for the condensate film coefficient to deduce a value for the scale resistance. The scale formation thus introduced another unknown, the scale resistance, such that it was not possible to determine the value of the condensate film resistance from the experimental data directly.

Othmer and White [17], and Othmer and Berman [18] used a glass condenser and a 2-in.-diameter tube with nearly a zero vapor velocity boundary condition to measure the film coefficients. It was possible to view the condensation pattern through the glass condenser. The

results from these experiments for film coefficients of various alcohols and acetates are within 10 percent of the values calculated using Nusselt's equation. (The experimental measurements are compared with Nusselt's solution in figures 7, 8, and 9 of reference 18). These results, however, show a decrease in $h/h_{Nu}$ with increasing heat flux. Othmer and Berman observed a thicker film around the lower portion of the tube surface at higher condensation rates as a result of the presence of more droplets. This condition is referred to as the so-called "screening effect" which means that the drop formation results in a thicker condensate film than that predicted theoretically by Nusselt.

Henderson and Marchello [10] reported that the Nusselt equation describes the problem adequately except at the region near the bottom of the tube where thickening of the film and droplet breakoff occurs. For this effect they decided to add a correction factor to the Nusselt equation. The dimensionless group used was the Ohnesorgenumber, $\mu/[\rho g D\sigma]^{1/2}$. They correlated data from seven different experimental studies with respect to the Ohnesorge number. The scatter of experimental data from the Ohnesorge correlation was still as high as 40 percent. It should also be realized that most of the correlated data are subject to deviations due to differences in the condensation patterns besides the surface tension effects at the tube bottom.

Chen [19] solved the boundary layer equations of momentum and energy for the case of laminar film condensation on a horizontal tube.

In this analysis the inertia terms were included in the momentum equation and the convection terms were included in the energy equation. The zero vapor velocity assumption was used outside of the vapor boundary layer. The major simplifying assumption of this analytical study was in neglecting the surface tension forces. The results deviated from Nusselt's solution only for a non-zero inertia effect parameter or a non-zero heat capacity parameter. The deviations increased as the Prandtl number changed from unity. For both the heat capacity parameter and the inertia effect parameter less than unity and Prandtl number close to unity, the solution obtained was different from Nusselt's solution only in the numerical constant which was 0.728 instead of Nusselt's 0.725.

The prime consideration in the present experimental study is on the effects of surface tension on the heat transfer coefficient in film condensation on horizontal tubes. When the system geometry is small, the heat capacity and the acceleration effect parameters are generally sufficiently small so that the two-dimensional solution to the problem is represented by Nusselt's equation. The flow pattern at the small geometries, however, deviates from the two-dimensional pattern as a result of surface tension forces at the liquid-vapor interface. The purpose of the present investigation is to consider the effect of flow pattern transition from a near two-dimensional to three-dimensional on the heat transfer in film condensation on horizontal tubes. For this purpose it was decided to conduct experiments on tubes of different small diameters under nearly the same boundary conditions. Attention

was also given to observe the exact condensation pattern and to eliminate scale effects in order to obtain repeatable experimental results. The measurement technique used is an indirect method originally suggested by Wilson [20] and later discussed in reference 8.

## II. EXPERIMENTAL APPARATUS AND PROCEDURE

### Equipment

The experimental facility, as shown in Figures 1 and 2 consisted of a condenser, steam and water supply and control systems, and temperature measuring instrumentation. The condenser shell was constructed from a 2 ips one-ft-long black iron pipe section flanged to a pyrex section of the same length and diameter. Steam inlet and condensate exit pipes of 3/4 ips were welded to the iron pipe condenser section. The ends of the condenser were flanged. The test section assembly connections to the condenser were designed with tube fittings to provide for quick mounting and removal of the test section assembly. Steam pressure was measured by a bourdon-tube pressure gage. Steam temperature was measured by a copper-constantan thermocouple inserted into the condenser. Cooling water was obtained from the building supply line and the flow rate was controlled by manual adjustment of the throttling valve. A full-view glass tube rotameter (Brooks Model 1112A08N3B1A) was used for the measurement of cooling water flow rates. Water from the rotameter entered the test section located in the condenser and was discarded after exiting from the test section. Saturated steam entered the condenser and the condensate was removed by a steam trap.

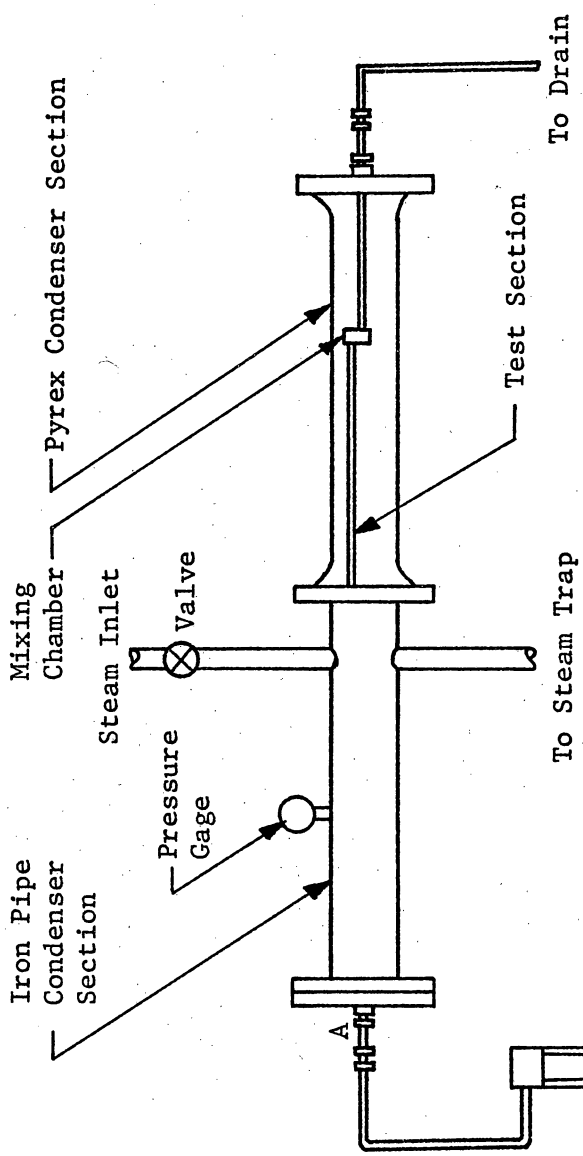


Figure 1. Arrangement of the Equipment.

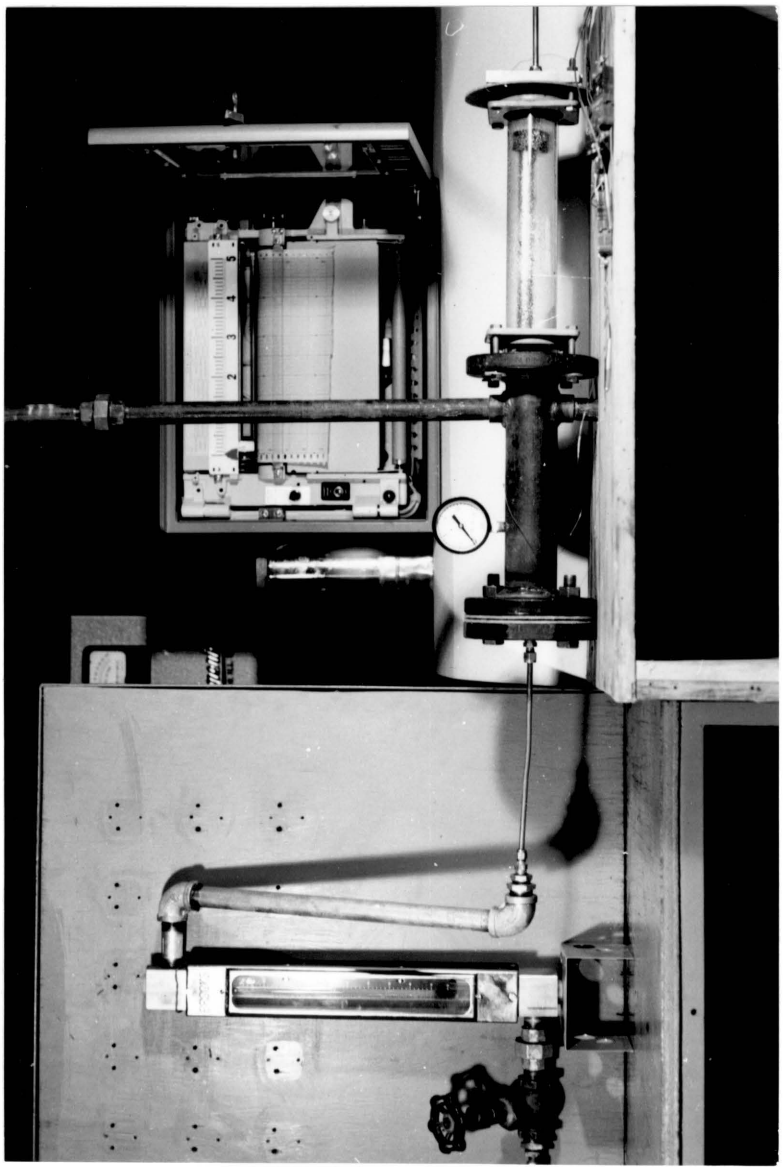

Figure 2. Picture of the Equipment.

The test section assembly was connected to the cooling water line from the rotameter by tube fitting A. A pictorial diagram of the test section assembly is shown in Figure 3. For measuring the bulk temperatures of the cooling water, mixing chambers were placed at the test section inlet and exit. The mixing chamber geometry was so arranged that the incoming stream impinged on the wall of the chamber before leaving the chamber. Test section inlet and test section exit thermocouples were placed into the mixing chambers through a hole drilled in the chamber wall, and sealed by soldering. The mixing chambers, the cooling water inlet tube, and the cooling water exit tube were insulated by 1/16 in. thick cork on the outside and completely sealed with caulking (Figure 4). The insulation served to eliminate heating through the mixing chamber walls and also eliminated conduction into the mixing chambers along the cooling water inlet, and exit tubes. Five test section assemblies were prepared with different test section diameters. The test section dimensions are given in Table I.

The thermocouples used in the experiment were all copper-constantan, bulk "Xactpak" with MgO insulation (Claud S. Gordon Company), with a specified accuracy of $\pm$ 3/2 deg F. For accurate determination of the heat transfer rates, the mixing chamber thermocouples were calibrated against a certified platinum resistance temperature sensor (Rosemount Engineering Company, Model 104MB24ABCC) to $\pm$ 0.1 deg C for three points over the range 25 deg C to 75 deg C. The calibration curves are given in the Appendix. The thermocouples were connected to a

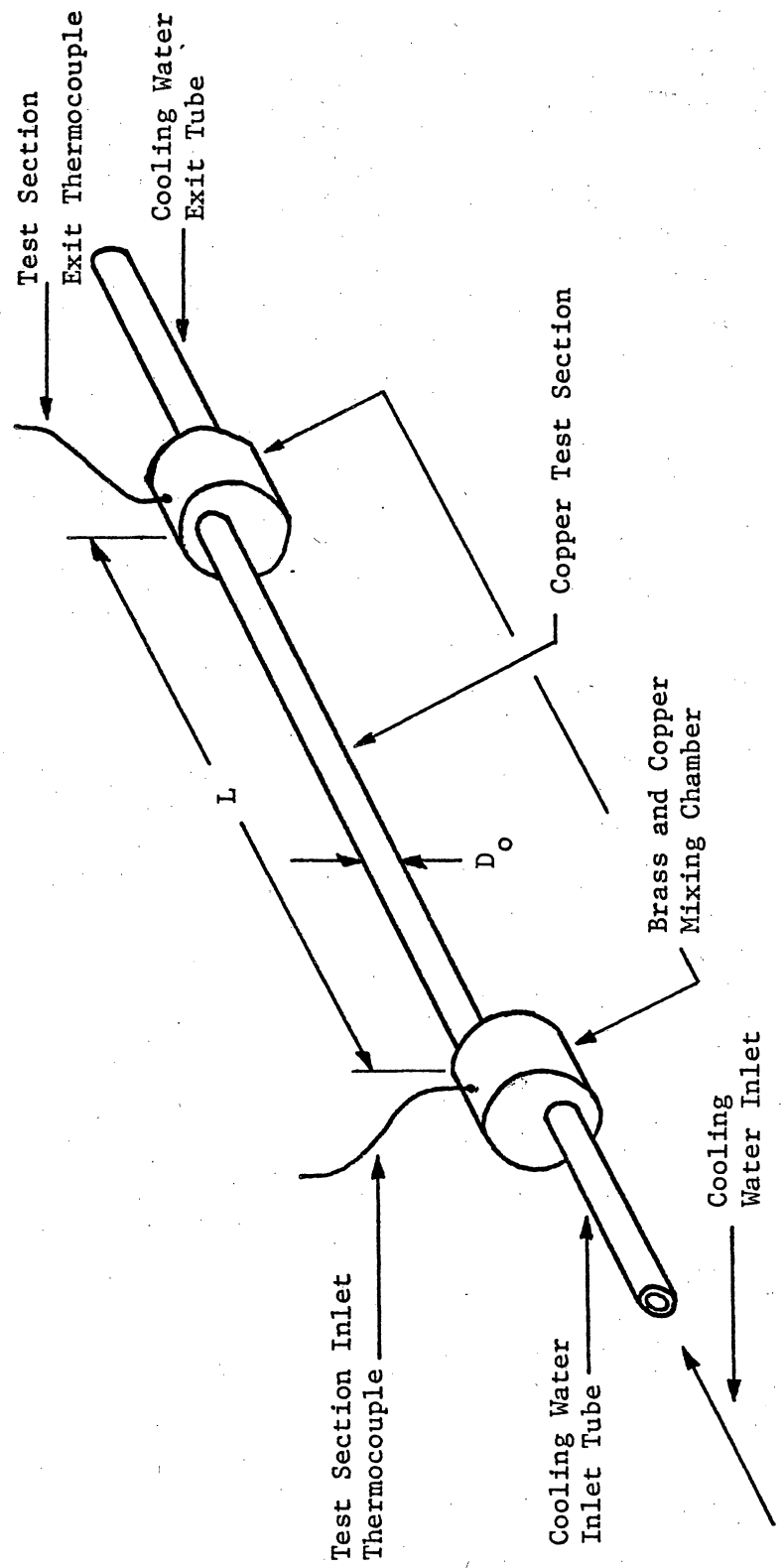


Figure 3. Pictorial View of the Test Section Assembly.

Figure 4. Mixing Chamber and Cooling Water Exit Tube Insulation.

TABLE I. Test Section Dimensions

| Test Section Assembly No. | $D_o$ (in.) | $D_i$ (in.) | L (in.) |
|---|---|---|---|
| 1 | 0.122 | 0.070 | 10.0 |
| 2 | 0.182 | 0.110 | 18.0 |
| 3 | 0.250 | 0.180 | 18.0 |
| 4 | 0.375 | 0.300 | 18.0 |
| 5 | 0.625 | 0.565 | 20.0 |

multipoint Honeywell recording potentiometer. An ice bath was used as the cold junction. The cold junctions were coated with electrical insulation and placed in glass tubes to prevent stray currents between the junctions. Prior to the start of the experiment, the Honeywell recording potentiometer was calibrated by adjusting the resistor location with a Honeywell standard cell. After this setting, the potentiometer recordings were checked at 1 mv increments over the 5 mv span of the recorder chart using the Honeywell standard cell and the precision resistance circuit from another Honeywell potentiometer. The smallest division on the recorder chart was in 0.02 mv increments and the recordings were readable within $\pm$ 0.005 mv.

The flowmeter was calibrated by directly measuring the mass flow of water over periods of time. This calibration was insensitive to changes in water temperature over the temperature range encountered in the experiments. The pressure gage was calibrated using a dead-weight tester (The Schaeffer & Budenberg Manufacturing Company). The calibration charts are presented in the Appendix.

Numerous preliminary runs were conducted to determine the general characteristics of the experiment setup and to observe the condensation pattern on the test section. Before each experimental run, tap water from the main was allowed to flow until a steady state condition was reached in the cooling water temperature. This was necessary because the water in the building water pipes was initially close to room temperature and higher than the temperature of water in pipes outside the building. Once this steady state condition was reached, the inside of the test section was flushed with diluted sulfuric acid. This

internal cleaning procedure was initially done to every test section and before each run to eliminate scale formation inside the test section. In the later runs, however, no difference was observed in the heat transfer results when this procedure was not followed. Clearly internal scale formation was not a rapid process. Special attention was given to the cleaning of the test section condensation surface. Scale or dirt was removed from the surface by washing and gently applying emery paper to the surface. After the surface was washed, magnesium metal powder was applied to the surface and the surface was thoroughly washed again. This resulted in a clean, smooth, and shiny surface that was readily wetted by cold water. The test section was then mounted in the condenser and the throttling valve turned on to introduce clean tap water into the system. The condensation surface cleaning procedure was repeated before each experimental run. Next, steam was let into the condenser by the valve on the steam line. Before starting to take data, air was removed from the condenser by letting steam flow out of the system for approximately 30 sec. This was done by removing the gage to bleed the air out.

The system was then ready for experimental measurements. Data were taken at five different cooling water flow rates in the turbulent region for each run. The quantities measured were: cooling water flow rate, steam pressure, steam temperature, test section inlet water temperature, and test section exit water temperature. Because of the small dimensions of the system, the steam rates necessary for condensation were very small and the boundary conditions were essentially that

of negligible axial steam velocity and constant steam temperature in the condenser.

A generalized computer program with plotter output was used to process the data. The following section gives the basic calculation procedure for reducing the experimental data used in the computer program.

Data Reduction Procedure

The electrical thermal analogy principle was used to deduce heat transfer results from experimental data. Thermal resistance is defined as the reciprocal of heat conductance, U. An equation similar to Ohm's law in electric-circuit theory for heat flow rate is

$$q''_w = \Delta T/[1/U].$$

The following is an outline of the calculation procedure:

1. Mean temperature difference, $\Delta T$

$$\Delta T = [T_1 - T_2]/\ell n \quad \{[T_s - T_2]/[T_s - T_1]\}$$

2. Total heat transfer, q

$$q = cm[T_2 - T_1]$$

3. Total thermal resistance, $R_t$ (ordinate in Wilson's plot)

$$R_t = \Delta T/q$$

(Wilson's plot is discussed in detail in Appendix I)

4. Average cooling water velocity, V

$$V = 4m/[\pi \rho D_i^2]$$

5. Abscissa in Wilson's plot, X

$$X = [1/V]^{0.83}$$

6. Five sets of $(X,R_t)$ values were calculated corresponding to each set of data and a least squares curve was fitted to obtain

$$R_t = a + bX$$

7. Tube wall thermal resistance, $R_w$

$$R_w = \ell n[D_o/D_i]/[2\pi k_w L]$$

8. Condensate film thermal resistance, $R_o$

$$R_o = a - R_w$$

9. Internal flow thermal resistance, $R_i$

$$R_i = bX$$

10. Test section outside wall temperature, $T_{w,o}$

$$T_{w,o} = T_s - qR_o$$

11. Test section inside wall temperature, $T_{w,i}$

$$T_{w,i} = T_{w,o} - qR_w$$

12. Internal Prandtl number, $Pr_2$

$$Pr_2 = c\mu(T_2)/k(T_2)$$

13. Internal Reynolds number, $Re_2$

$$Re_2 = 4m/[\pi D_i \mu(T_2)]$$

14. Calculated internal Nusselt number, $Nu_{i,c}$

$$Nu_{i,c} = 0.0155\ Pr_2^{0.5}\ Re_2^{0.83}\ [1 + 6D_i/L]$$

15. Measured internal Nusselt number, $Nu_{i,m}$

$$Nu_{i,m} = 1/\left[\pi LR_i[k(T_1) + k(T_2)]/2\right]$$

16. Average inside wall temperature, $T_{w,i,a}$

$$T_{w,i,a} = \sum T_{w,i}/5$$

17. Average outside wall temperature, $T_{w,o,a}$

$$T_{w,o,a} = \sum T_{w,o}/5$$

18. Average steam temperature, $T_{s,a}$

$$T_{s,a} = \sum T_s/5$$

19. Average condensate film temperature, $T_{f,a}$

$$T_{f,a} = [T_{s,a} + T_{w,o,a}]/2$$

20. Average heat flux at outside surface, $q''_w$

$$q''_w = [\sum q/5]/[\pi LD_i]$$

21. Calculated film Nusselt number, $Nu_{f,c}$

$$Nu_{f,c} = 0.725\ \left[\rho^2 g\lambda(T_{f,a})D_o^3/\mu(T_{f,a})k(T_{f,a})\right.$$
$$\left.[T_{s,a}-T_{w,o,a}]\right]^{1/4}$$

22. Measured film Nusselt number, $Nu_{f,m}$

$$Nu_{f,m} = 1/[\pi LR_o k(T_{f,a})]$$

23. Ohnesorge number, $N_{Oh}$

$$N_{Oh} = \mu(T_{f,a})/[\rho g D_o \sigma(T_{s,a})]^{0.5}$$

24. Dimensionless number, $N_d$

$$N_d = 8\sigma(T_{s,a})/[\pi\rho g D_o^2]$$

25. Condensate film Prandtl number, $Pr_f$

$$Pr_f = c\mu(T_{f,a})/k(T_{f,a})$$

## III. DISCUSSION OF RESULTS

The first discussion in this section is on the sensitivity of Wilson's method to changes in the condensation pattern. A series of different condensation patterns observed in this study are discussed next. The Wilson's plots for the experimental runs are presented and the results are compared with the Ohnesorge correlation. Finally, a dimensionless number representing the ratio of the surface tension force to the gravity force is obtained to present the experimental results.

Figure 5 shows a Wilson's plot of one of the preliminary runs. The solid line is the curve fit for the experimental points. The broken line represents the curve fit for the points excluding the one at the lower cooling water flow rate. When the inside heat transfer coefficients are compared with the theoretical values it is seen that the broken line fit gives results in good agreement whereas the solid line fit gives much larger coefficients than the theoretical values. This discrepancy of heat transfer coefficients resulted from condensation pattern change. In this particular preliminary run, a decrease in the cooling water flow rate decreased the heat flux and the condensation pattern changed from film condensation into mixed condensation resulting in a lower resistance to heat transfer. The total resistance to heat transfer in all of the preliminary runs with mixed condensation were in all cases lower than the total resistances obtained under film condensation. Because of the lack of consistency

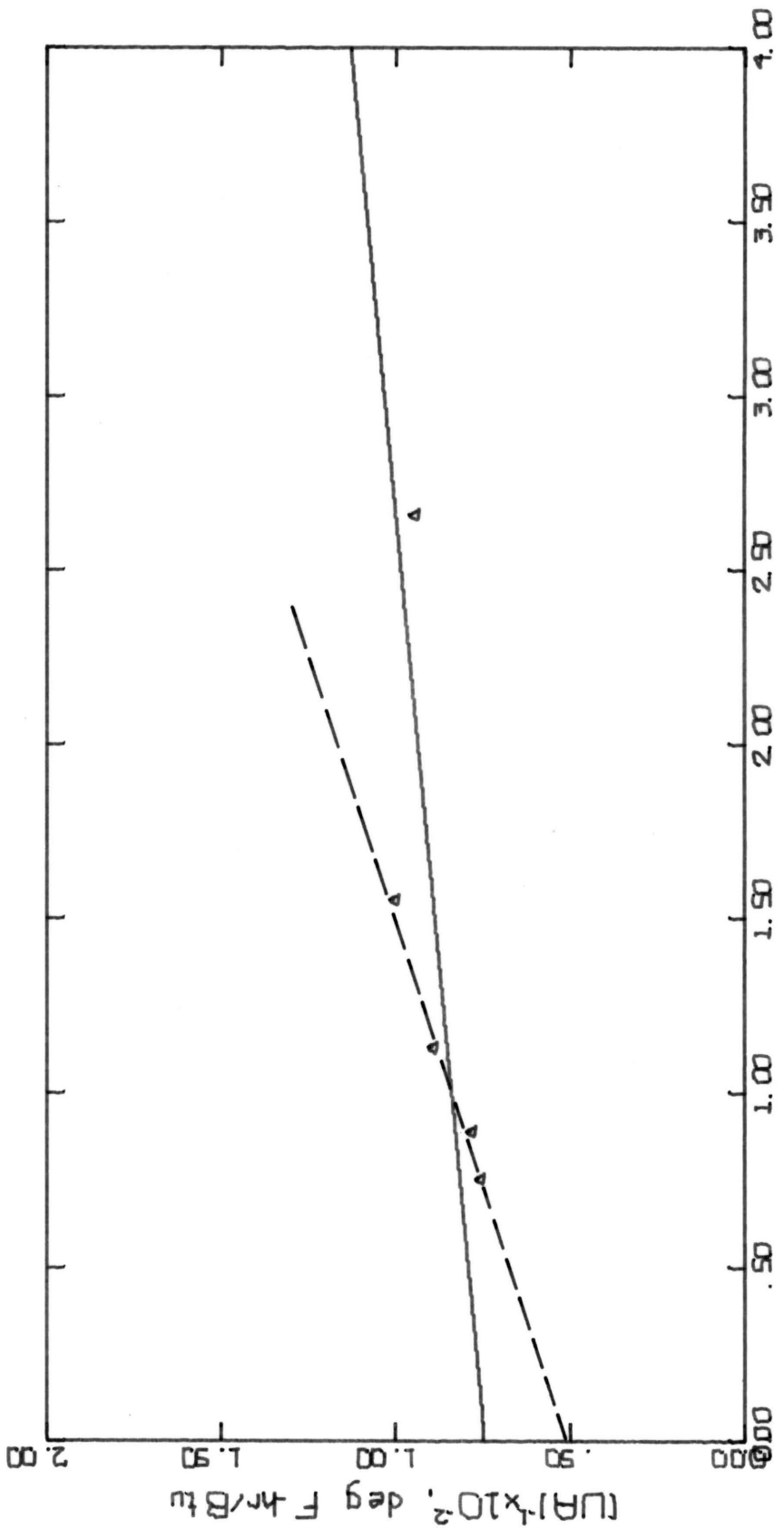


Figure 5. Wilsons Plot for Test Section No.3 A Preliminary Run

resulting from the condensation pattern change, the results of the preliminary runs were discarded.

Different condensation patterns on the test sections were observed in the experiments. When the test section surface was not carefully cleaned before placing it into the condenser, the condensate first appeared as a film on the surface. After approximately 15 minutes, areas of dropwise condensation began to appear on the surface. The condensation mode continued to change with time as more areas of dropwise condensation replaced areas of film condensation. The film condensation areas were adjacent to the dropwise condensation areas. The growing drops and the adjacent film coalesced rapidly. Figure 6 shows pictures of transitory condensation modes (mixed condensation) as dropwise condensation replaced film condensation. The entire transition shown in the figure took place in 15-30 minutes. The condensation pattern was not stable in the dropwise condensation mode and changed to a mixed condensation pattern after a period of time which ranged between 2 hours to 10 hours. This condensation pattern as shown in Figure 7 was stable for at least one week. The experiment was not kept in an operating condition for a period longer than one week. This final condensation pattern had dropwise spots surrounded by partial films. Areas that appeared to be free of liquid and not corresponding to either filmwise or dropwise patterns were observed on some parts of the surface.

The experimental measurements for which data are presented in Appendix IV were carried out with film condensation on the test section. The film condensation was obtained by the surface preparation procedure

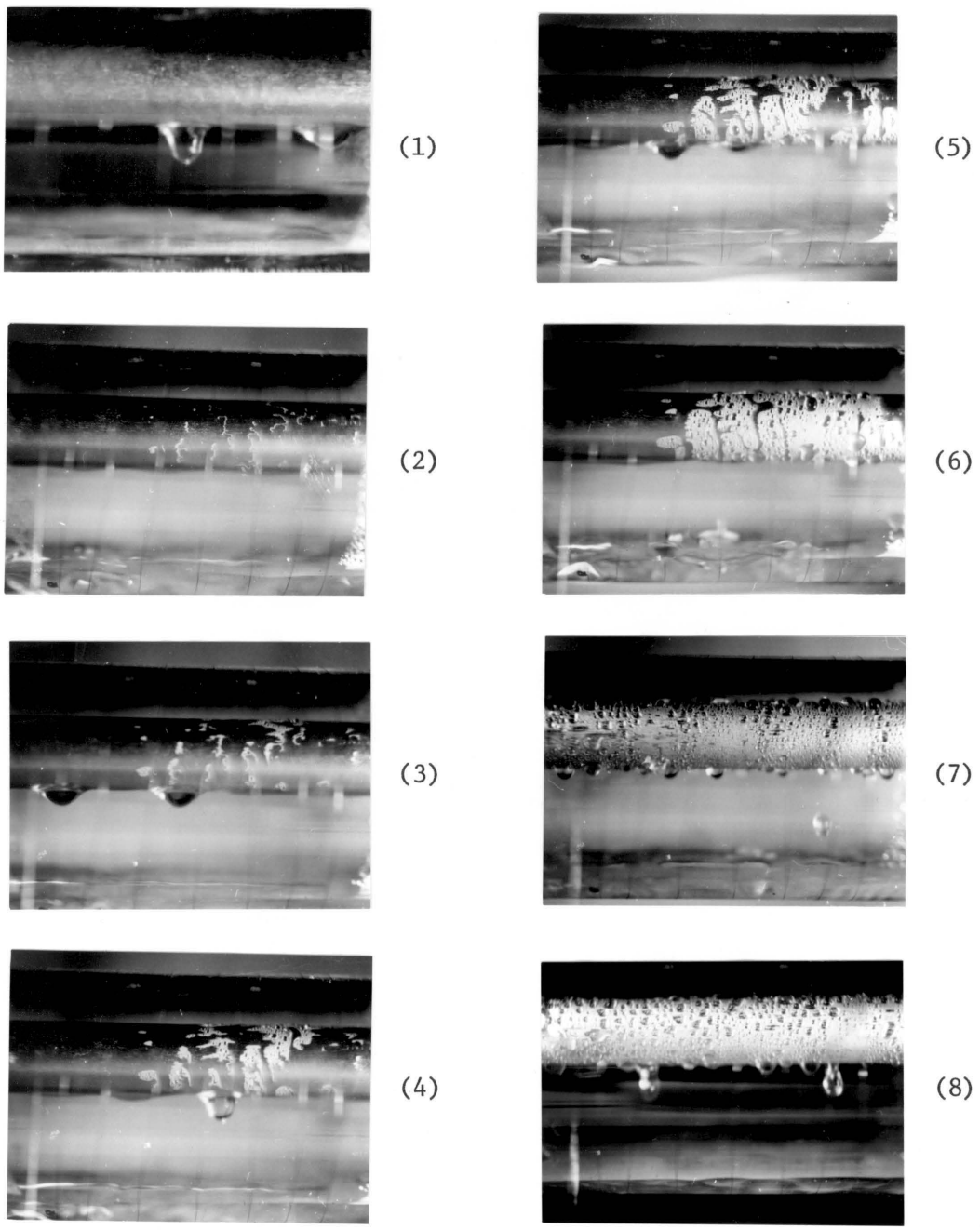


Figure 6. Transition from Film to Dropwise Condensation.

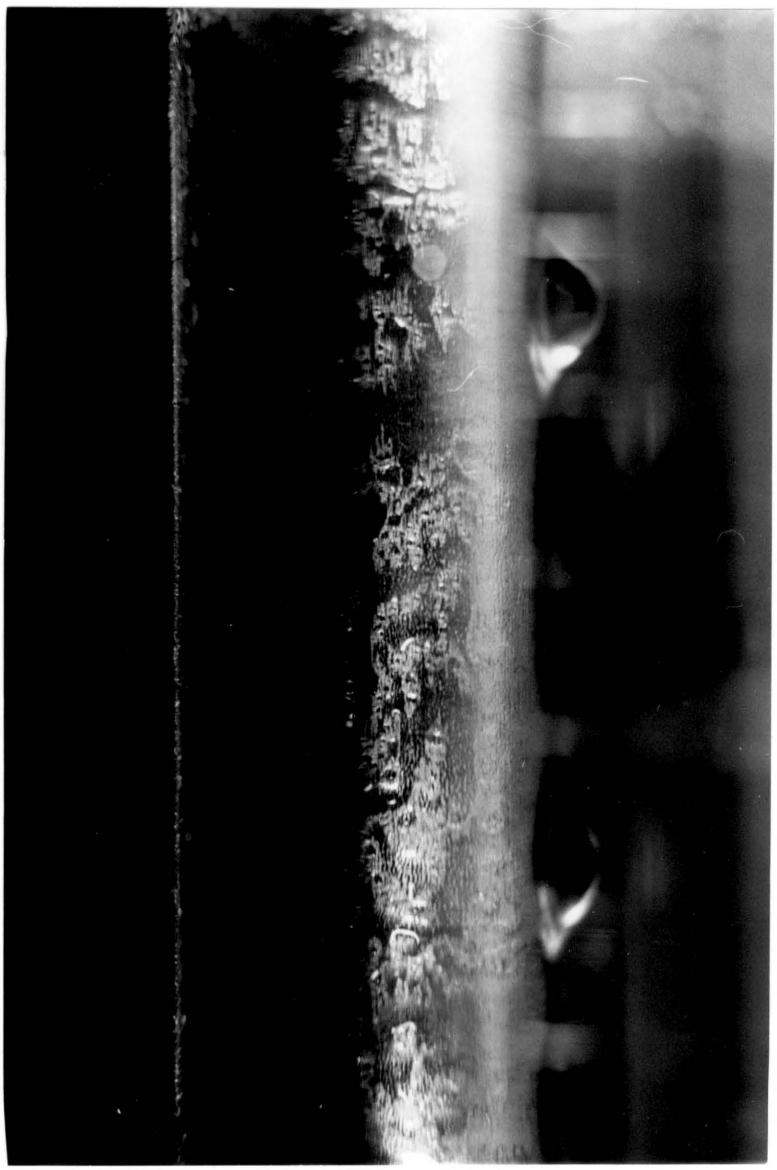

Figure 7. Mixed Condensation of Steam.

described in section II and was effective for 2-4 hours from the start of the experiment. All the measurements were made within this period. The transition from film condensation to mixed condensation appeared first near the exit end of the test section which corresponded to the region of the least local heat flux. The final form of condensation again was the mixed condensation pattern shown in Figure 7.

In some cases a condensation pattern in the form of streaks of condensate films of different thicknesses was observed. This condensation pattern is shown in Figure 8. Since the thicknesses of the condensate streaks cannot be determined by visual observation, there is the possibility that some parts of the surface were bare of liquid. If the streaks are films of different thicknesses with no bare parts on the condensing surface, the streaky flow pattern might be a wavy pattern induced by surface tension.

As a point of interest in drop formation dynamics, a picture of film condensation with symmetrically positioned drops is presented in Figure 9. This picture was taken after shutting the steam line off so that it represents the flow pattern as the heating rate approaches zero. The test section was very slightly inclined such that the drops were moving toward the right but maintaining the symmetry at the same time. The symmetry is lost at finite heating rates as a result of buildup and breakoff of the droplets.

Plots of the 14 experimental runs are presented in Figures 10-23. The experimental data and calculated parameters describing the experiment conditions are presented in Appendix IV. The measured internal Nusselt numbers are in excellent agreement with the theoretical values

Figure 8. Streaky Condensation of Steam.

Figure 9. Symmetry in Drop Formation at a Near-Zero Heating Rate.

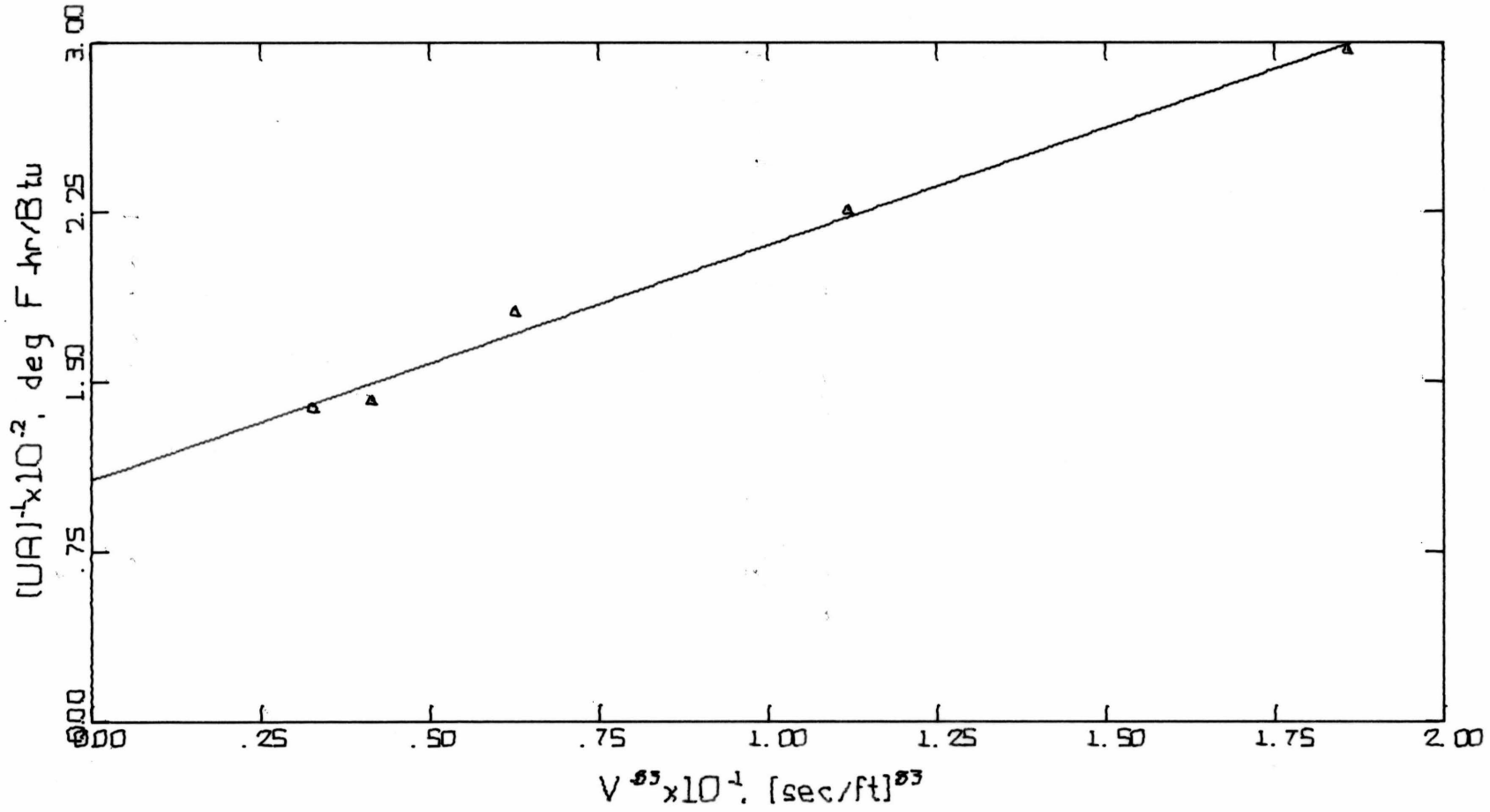


Figure10. Wilson's Plot for Test Section No. 1 Run No. 1

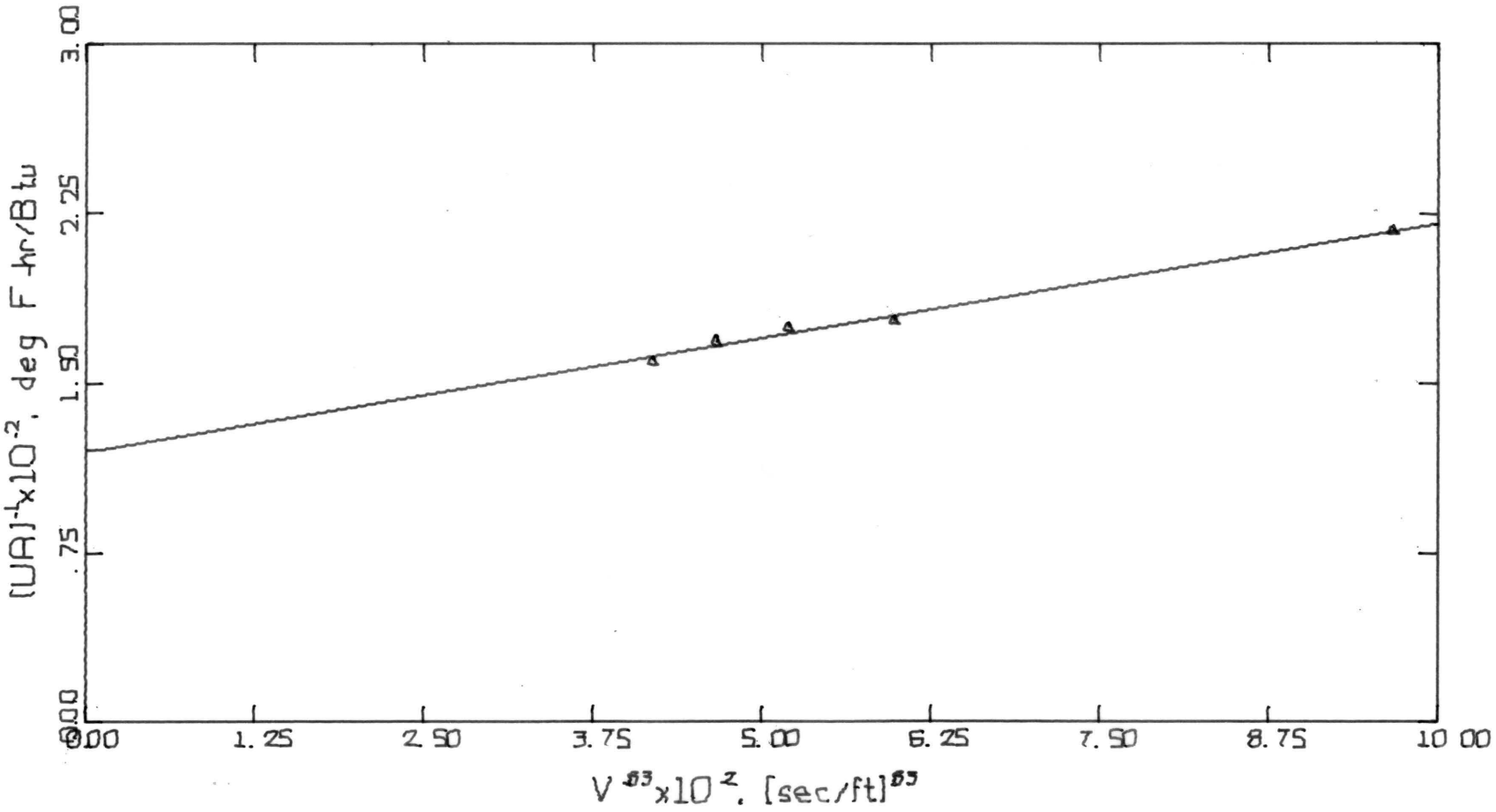


Figure 11. Wilson's Plot for Test Section No. 1 Run No. 2

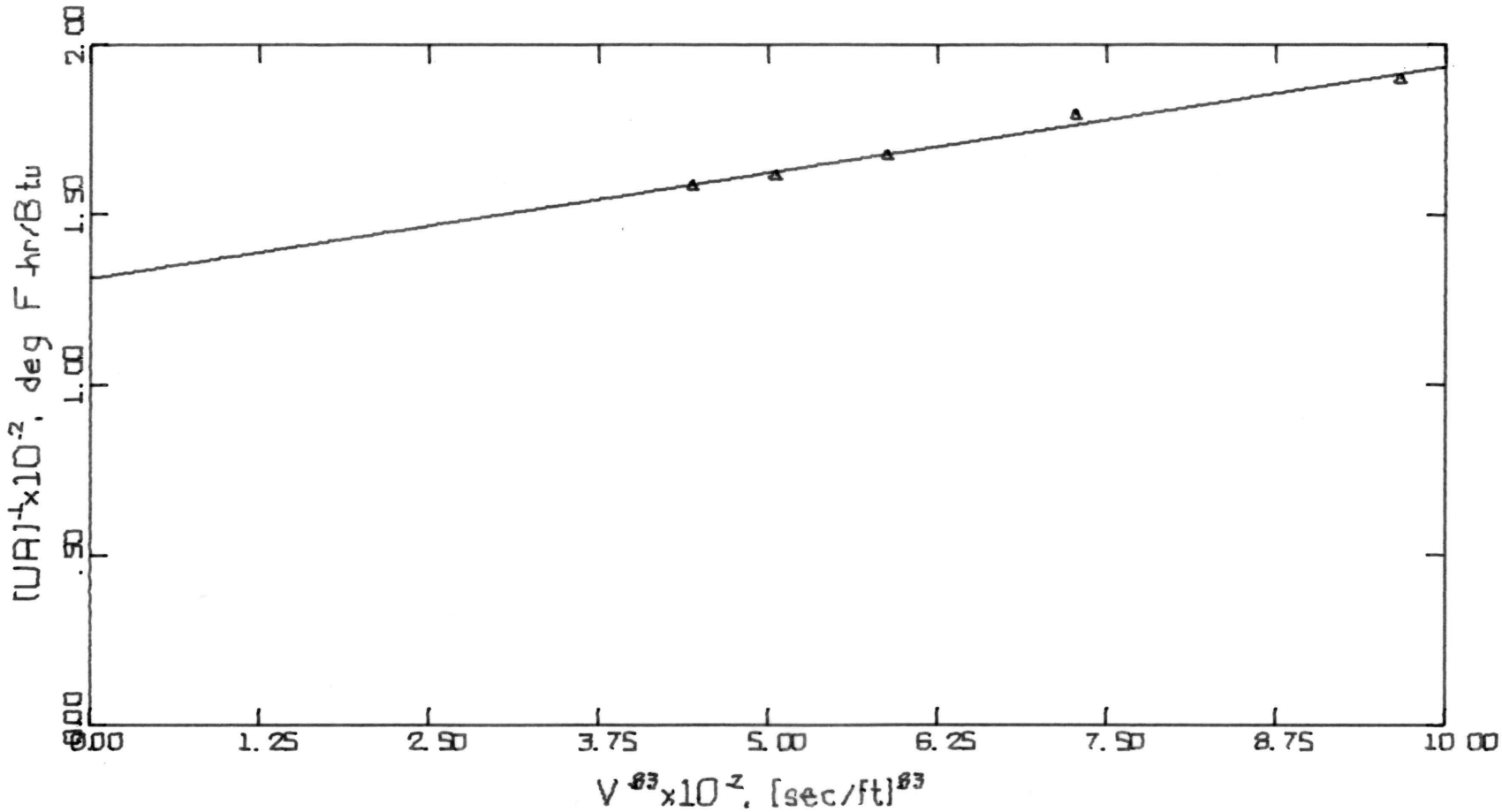


Figure12. Wilson's Plot for Test Section No. 1 Run No. 3

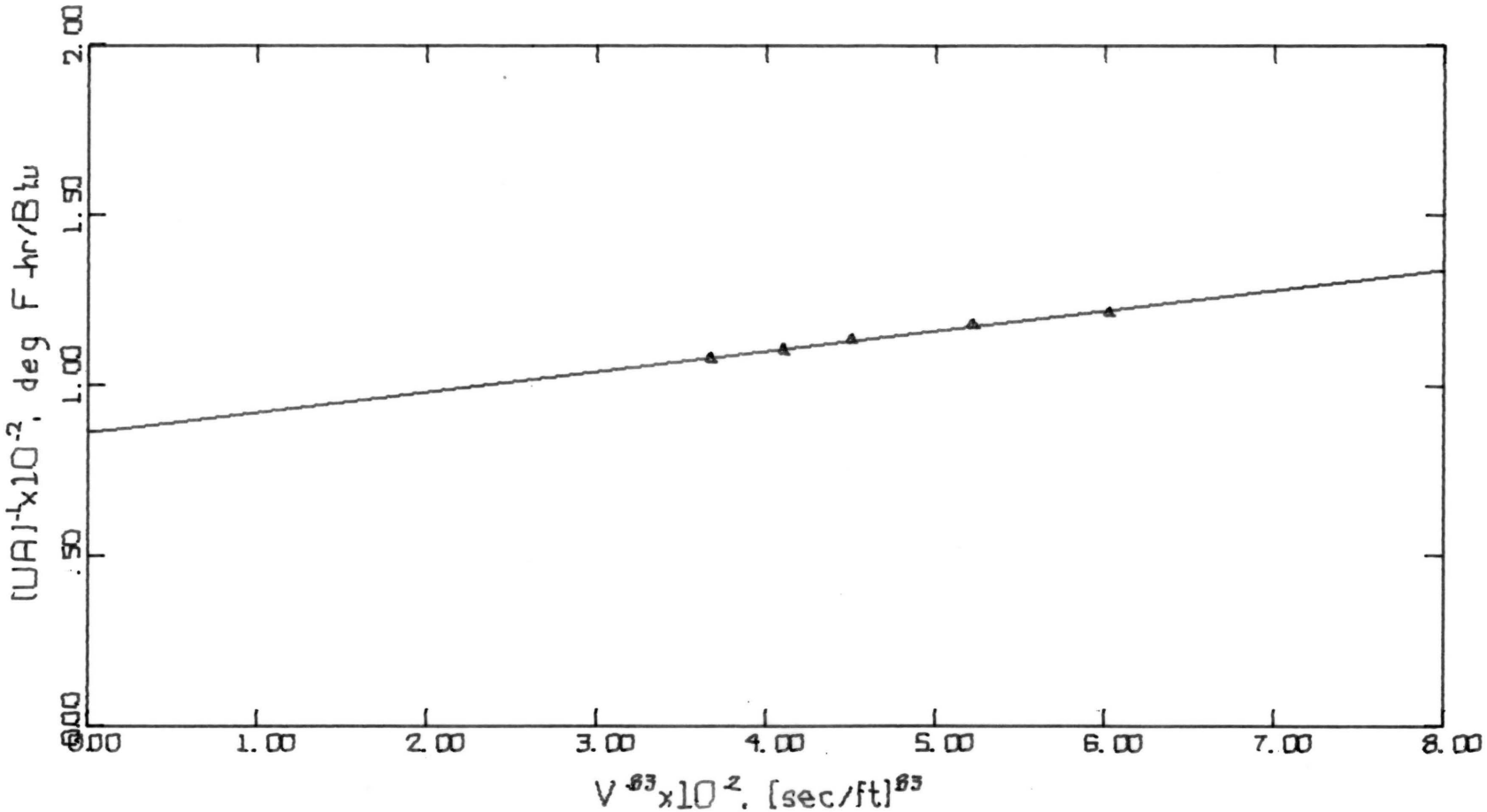


Figure13. Wilson's Plot for Test Section No. 2 Run No. 4

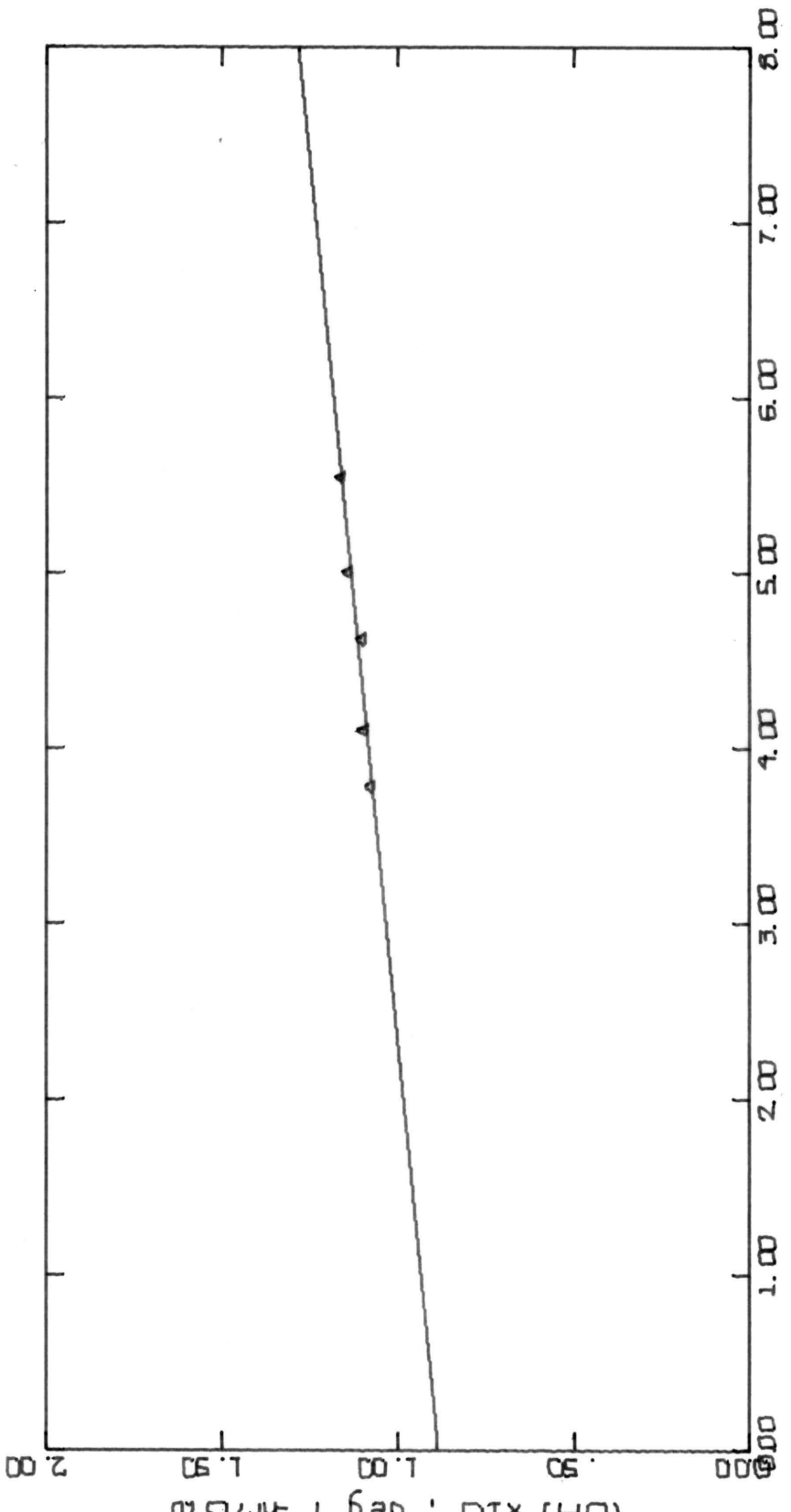


Figure 14. Wilson's Plot for Test Section No. 2 Run No. 5

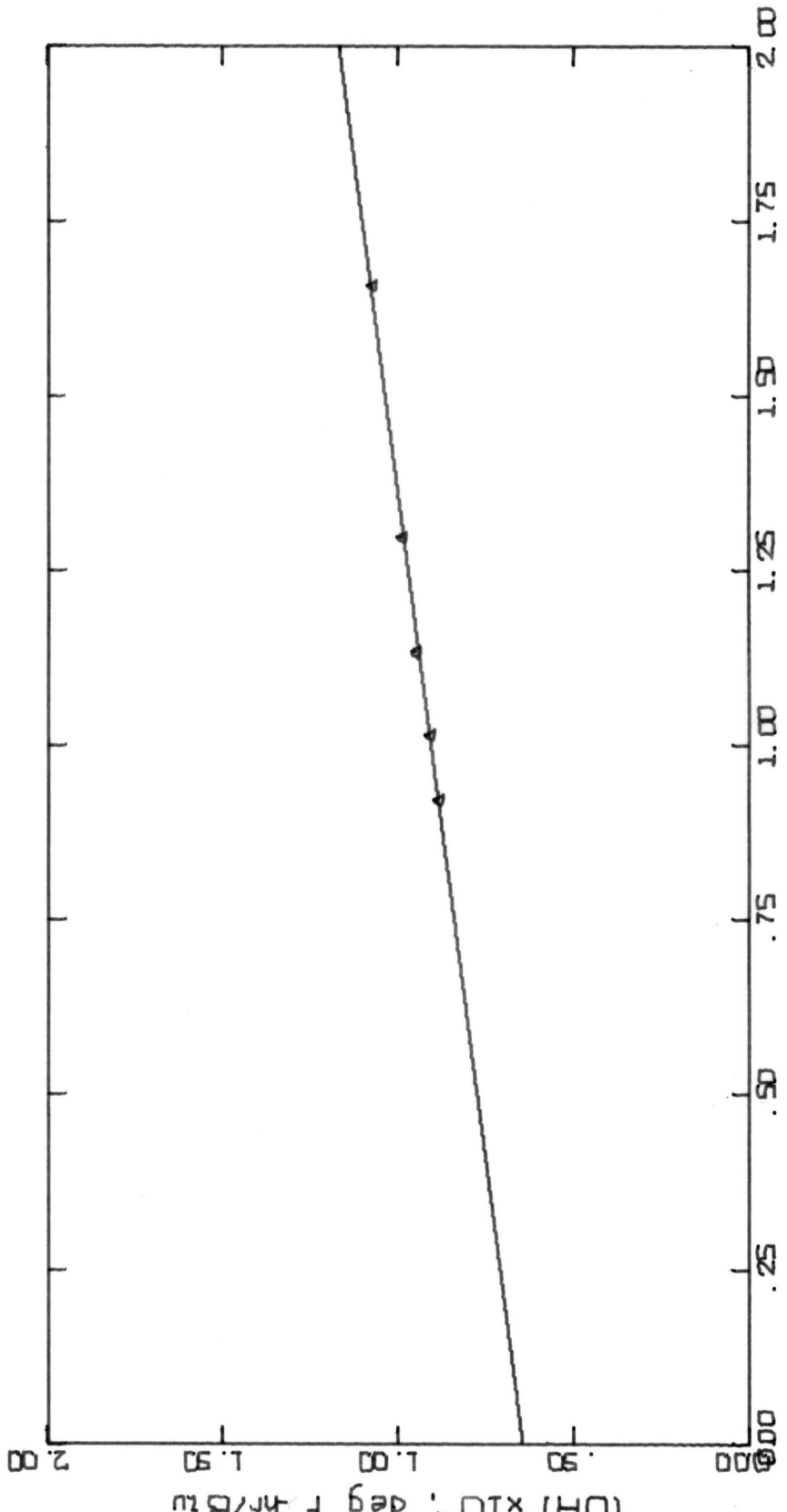


Figure15. Wilson's Plot for Test Section No. 3 Run No. 6

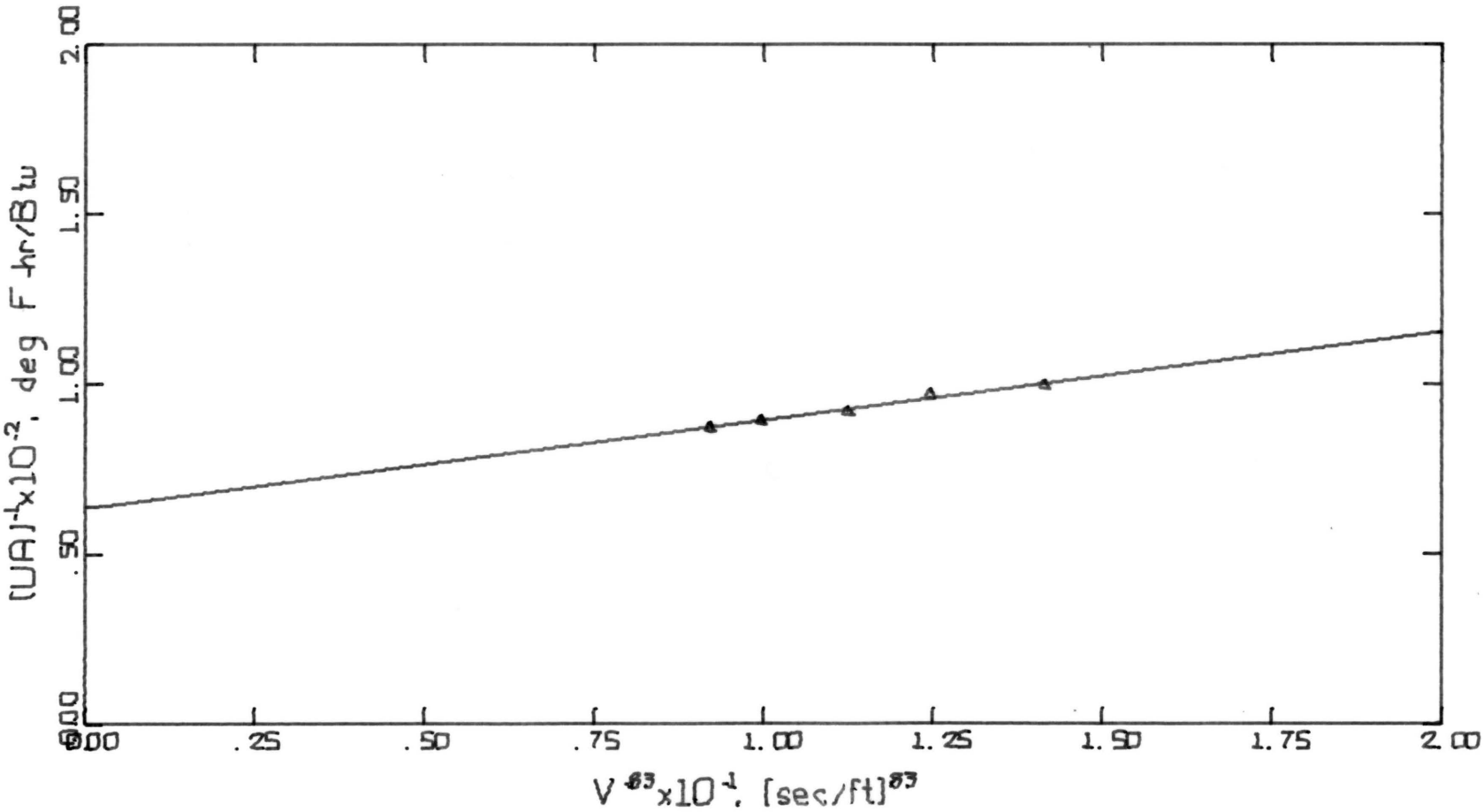


Figure16. Wilson's Plot for Test Section No. 3 Run No. 7

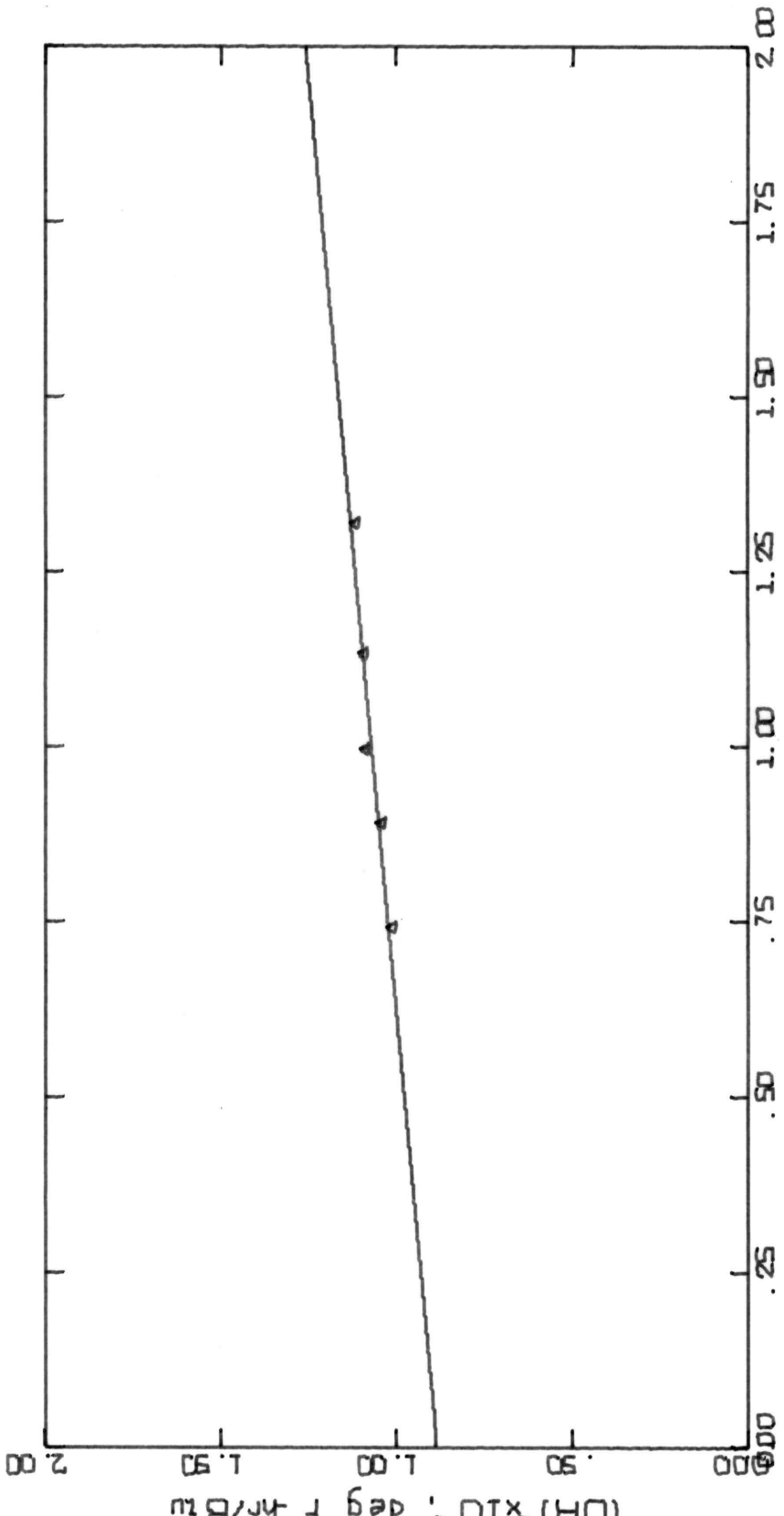


Figure17. Wilson's Plot for Test Section No. 3 Run No. 8

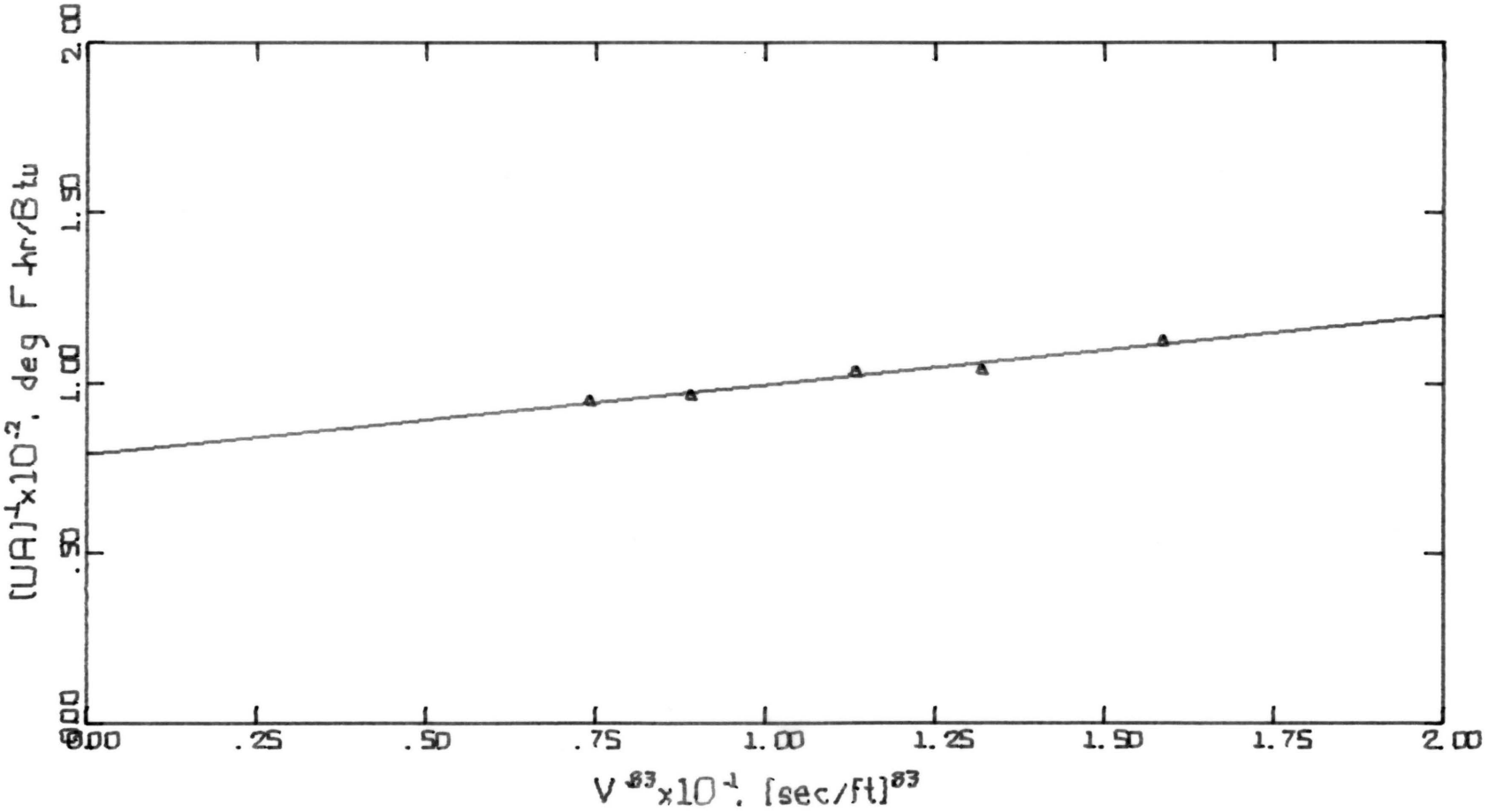


Figure 18. Wilson's Plot for Test Section No. 3 Run No. 9

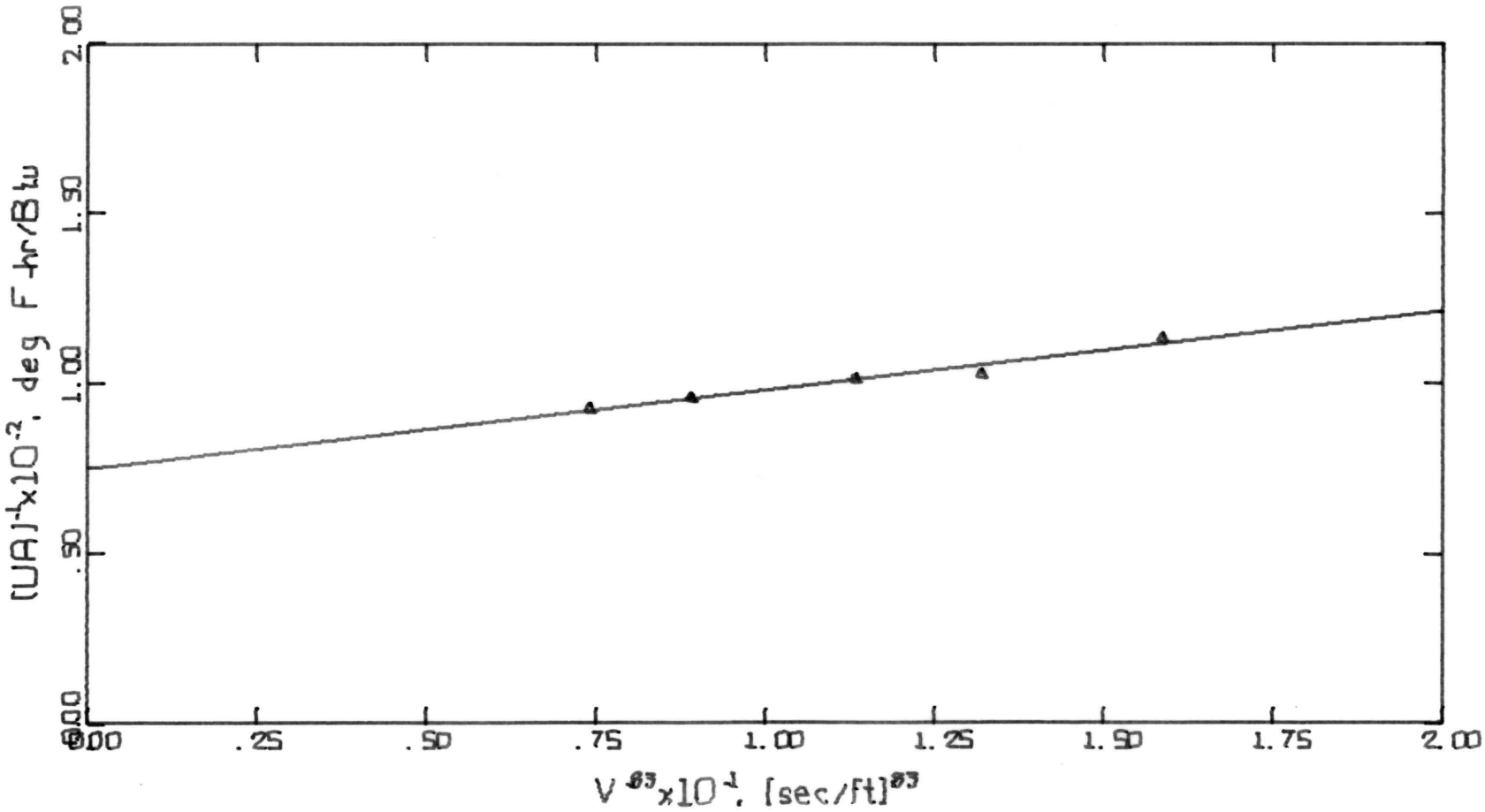


Figure 19. Wilson's Plot for Test Section No. 3 Run No. 10

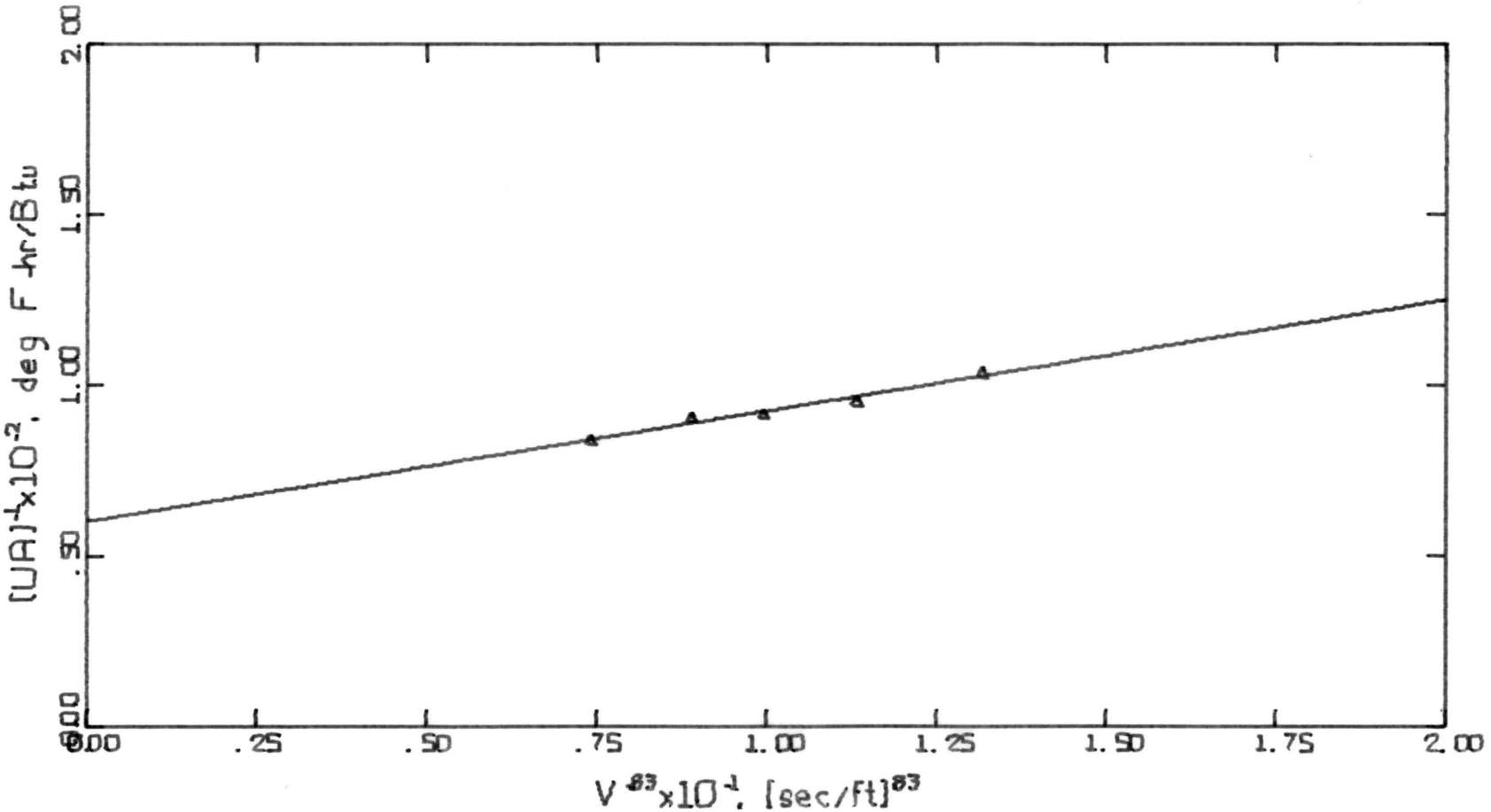


Figure 20. Wilson's Plot for Test Section No. 3 Run No. 11

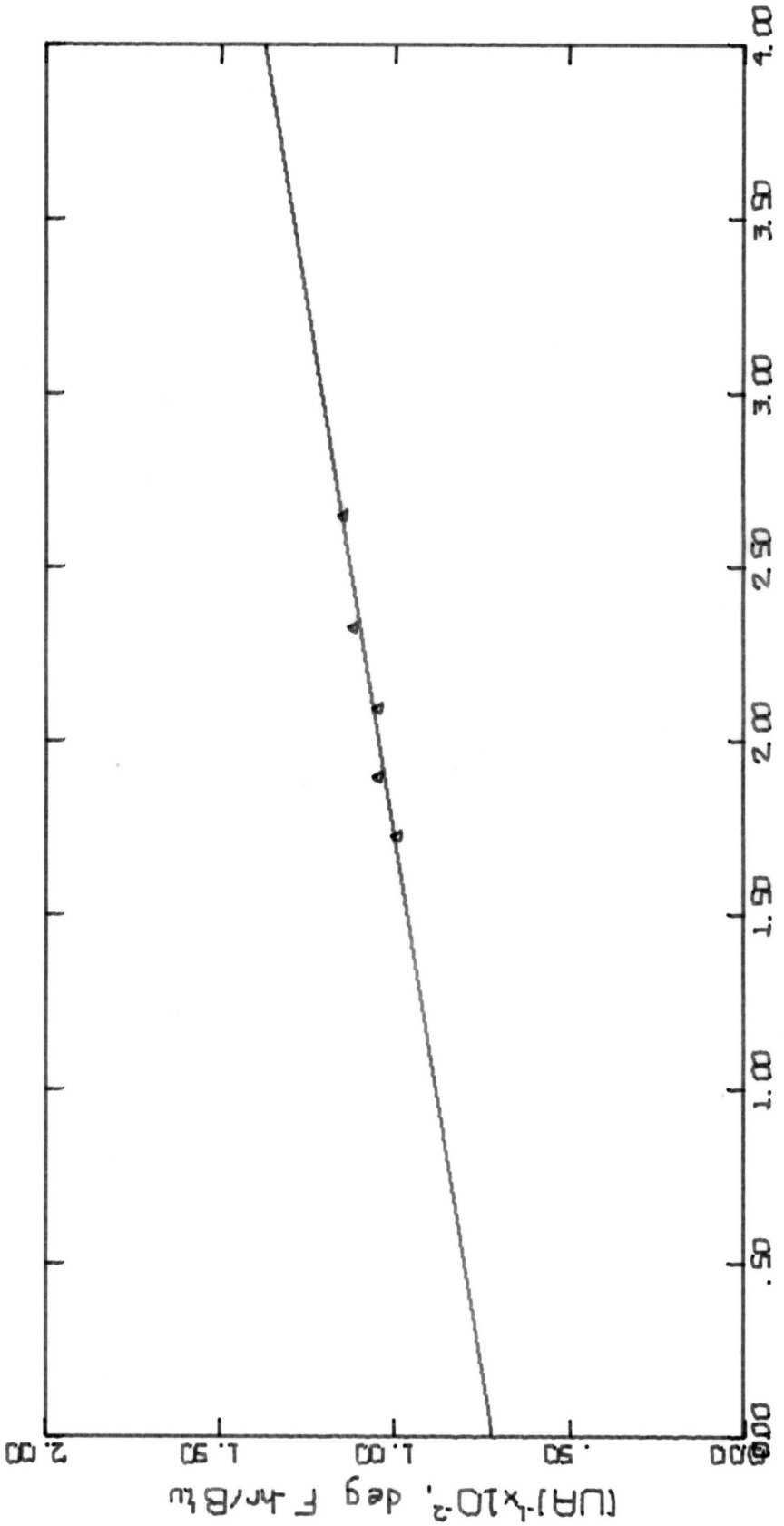


Figure21. Wilsons Plot for Test Section No. 4 Run No. 12

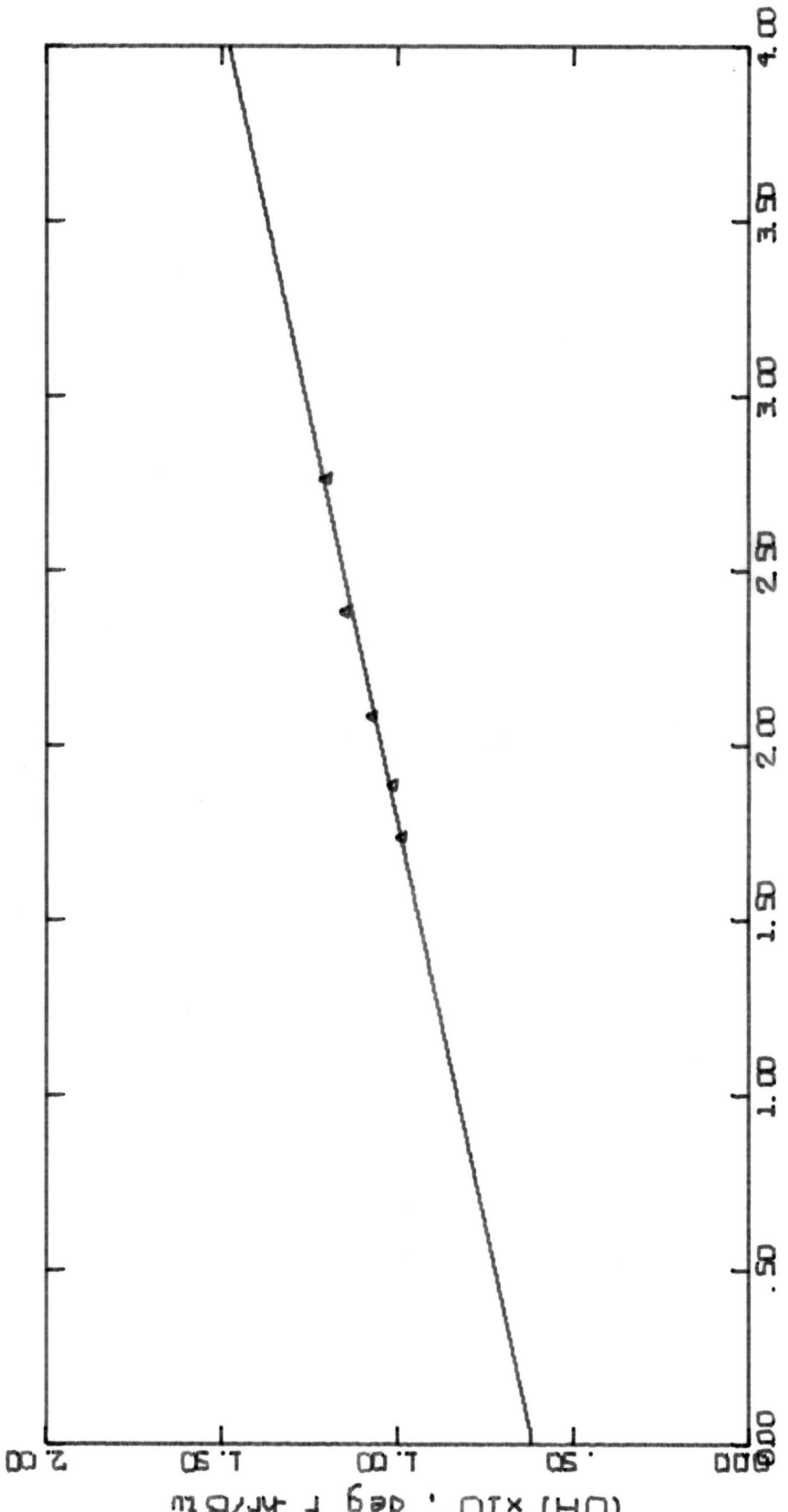


Figure 22. Wilson's Plot for Test Section No. 4 Run No. 13

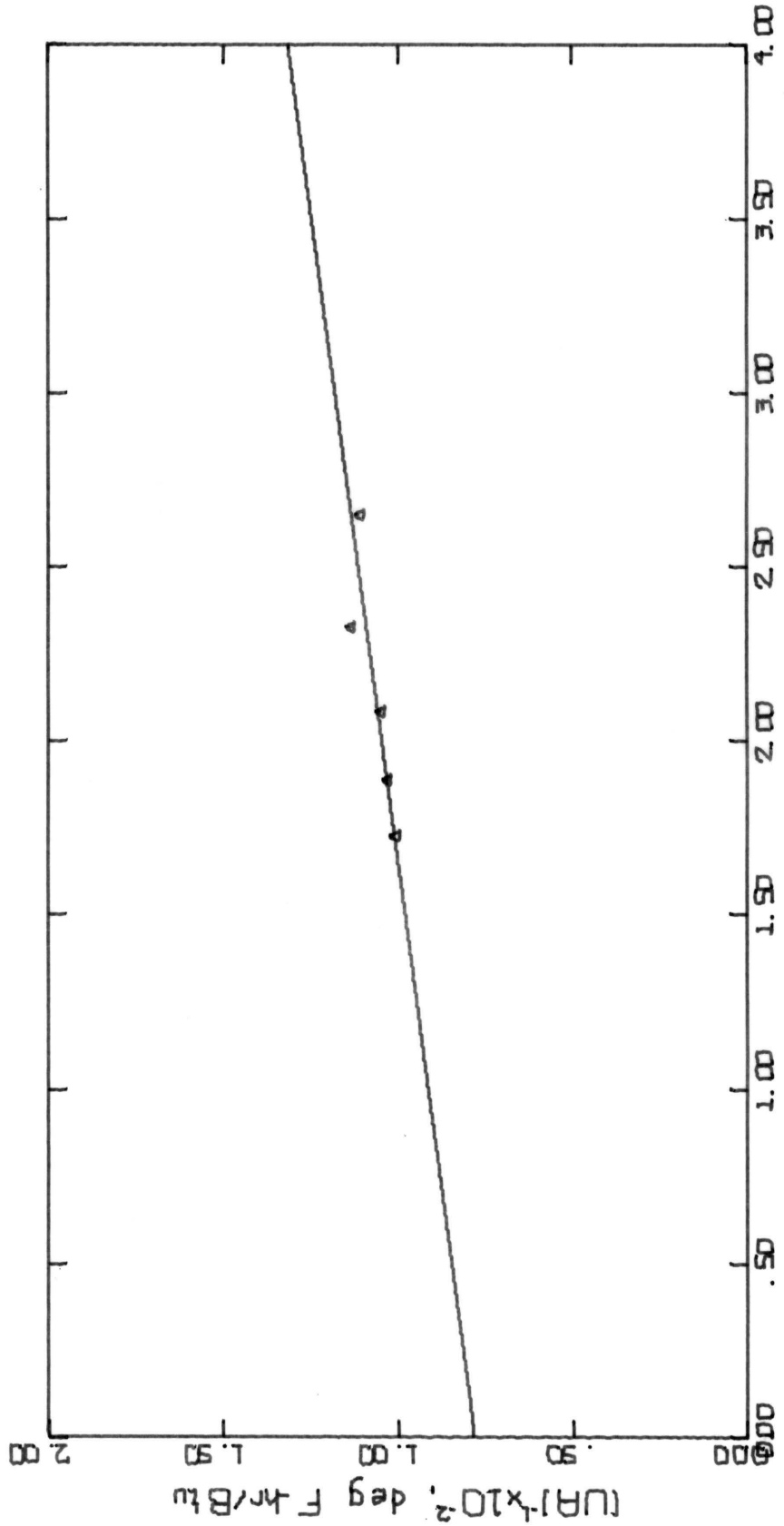


Figure 23. Wilson's Plot for Test Section No. 4 Run No. 14

in runs 1, 2, 5, 11, 13 and in fair agreement in the rest of the runs. Examination of the data and calculated parameters shows that in most of the experimental runs the condensate film resistance to heat transfer is several times larger than the internal resistance. The internal heat transfer results were therefore more sensitive to errors in experimentation than the condensate film heat transfer results. The error in condensate film Nusselt number measurement is expected to be on the order of the product of the error in the measurement of the internal Nusselt number and the ratio of the internal to condensate film resistances. It is observed from the data that the error deduced in this manner is less than 15 percent for the worst case. Since the ratio of the condensate film resistance to internal resistance is larger at smaller diameter tubes, measured film coefficients are more accurate at the smaller diameters.

The heat transfer results obtained using test section No. 5 showed a large deviation from theoretical results both for inside and outside Nusselt numbers. The design of the experimental apparatus and the fixed water line pressure for cooling water limited the internal Reynolds number for this test section to below 10,000. A Wilson's plot for reducing experimental data could not be used because the turbulent flow assumption was not good at the low Reynolds numbers. Also the internal resistance was greater than the outside film resistance which further complicated the experimental problems. The experiment for this test section was abandoned.

The ratio of the measured condensate film heat transfer coefficient to that calculated from Nusselt's analytical equation is plotted in Figure 24 with Ohnesorge number as the abscissa. The solid line represents the Ohnesorge correlation of Henderson [10,16]. It is clear that the present results are not correlated with the Ohnesorge number relationship. Furthermore, the heat transfer coefficient ratio shows an increasing behavior with increasing Ohnesorge number which is an opposite variation than that suggested by the Ohnesorge correlation. Henderson's Ohnesorge correlation was intended to account for the effects of surface tension and pipe diameter on the heat transfer coefficient. It is important to note, however, that the correlation was done for experimental data for which tube diameters were 0.625 in. and larger. His correlation therefore will not necessarily hold at the small tube diameters. A correlation will be developed later in this section for predicting condensation heat transfer on horizontal tubes under gravity and surface tension. It is necessary, however, to analyze the condensate droplet flow characteristics before going into the discussion of this correlation.

Pictures taken during film condensation on the test sections are shown in Figure 25. The condensate film flowing down the tube surface under gravity collects at the bottom of the tube in droplets because of the existence of surface tension. The flow pattern is time dependent and is three-dimensional rather than two-dimensional. The drop sizes for the smaller diameter tubes are of the order of the tube diameter. When the diameter of the tube is large, the condensate

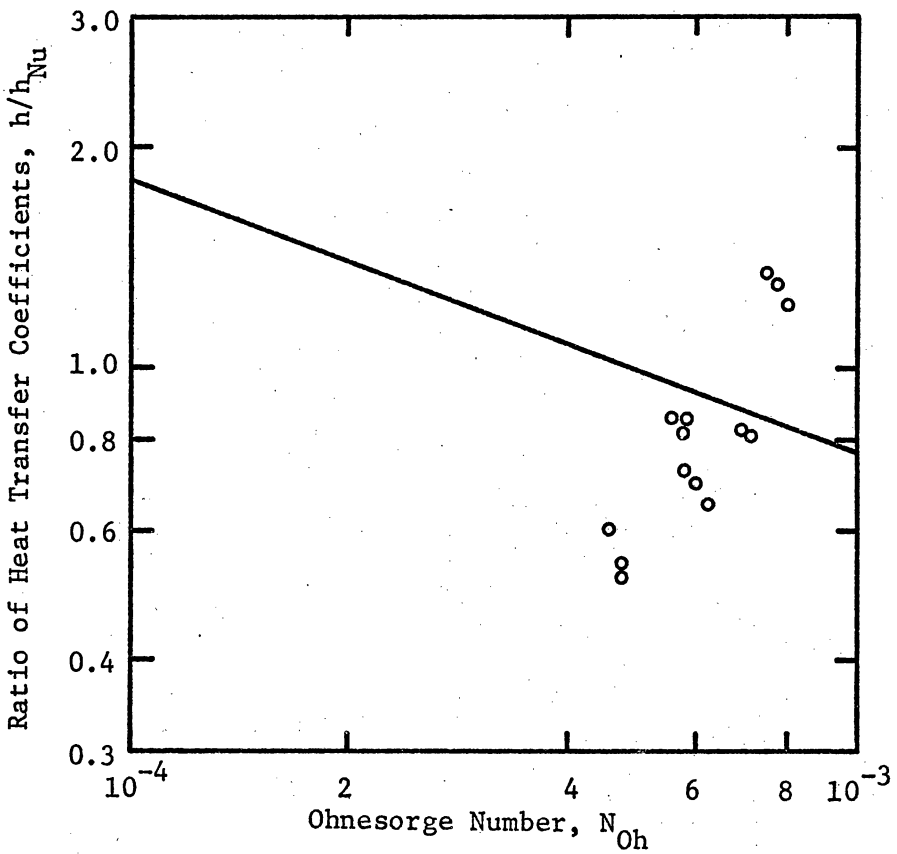


Figure 24. Comparison of Results with the Ohnesorge Correlation.

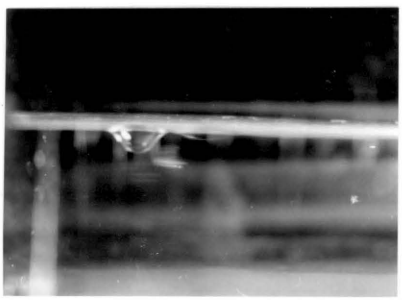

$D_o = 0.122$

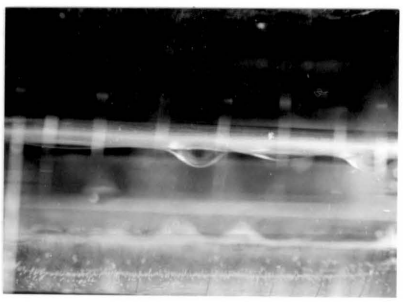

$D_o = 0.182$

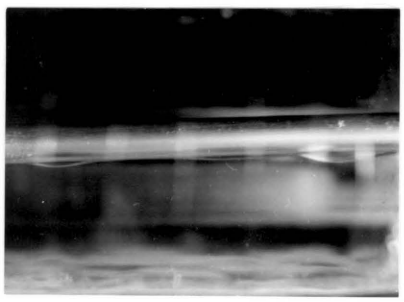

$D_o = 0.250$

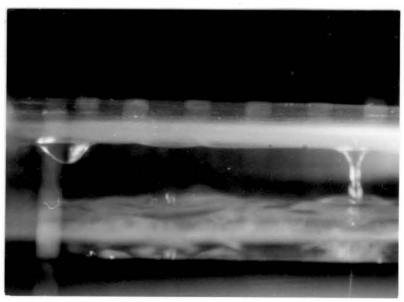

$D_o = 0.375$

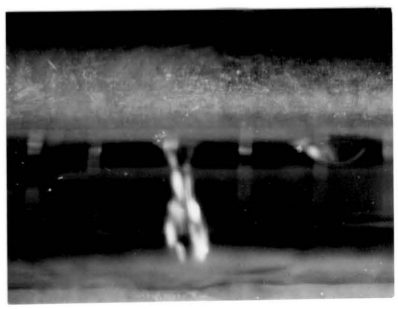

$D_o = 0.625$

Figure 25. Film Condensation on Horizontal Tubes.

flow rate is higher because of increased heat transfer rates. It is expected that condensate droplets will be dripping rapidly off the tube. The rate of condensation for smaller diameter tubes is lower since less heat is transferred and the time rate of dripping at the tube bottom is also lower. It was observed in this experiment through flow visualization that the rate of dripping decreased with decreasing tube diameter and at the smaller diameters 3-4 sec were necessary for a drop to build-up and leave the tube. Generally the test section had a small inclination with respect to the horizontal. This caused the drops to move in the direction of the inclination as they grew by collecting more condensate. At the small tube diameters, a drop moved 2-4 in. along the tube before it grew to a size large enough for dripping. A complete analytical treatment of the time dependent problem with surface tension is extremely complicated and was not attempted. In the following discussion, a dimensionless number representing the ratio of the surface tension force to the gravity force will be obtained from physical arguments.

It is shown in reference 19 that the temperature profile is linear in the condensate film for most applications in condensation heat transfer on horizontal tubes.[1] The heat transfer coefficient is

$$h = - k \left.\frac{\partial T}{\partial y}\right|_w / [T_w - T_s]$$

---

[1]Chen's analytical solution shows that the temperature profile is linear when $\xi<1$ and $\zeta\simeq 0$.

for a linear temperature profile

$$h = k/\delta$$

The heat transfer coefficient is determined by the conductivity and the thickness of the condensate film. An increase in average film thickness therefore will decrease the heat transfer coefficient and vice versa. Figure 26 shows the assumed flow geometry in the analytical solutions and the real flow geometry with condensate collection in form of a drop at the bottom side of the tube. The analytical solution of the problem should be expected to hold at large tube diameters when the flow pattern is essentially two-dimensional and the assumed flow pattern is close to the actual flow pattern. The film thickness is affected by the existence of the drops at the tube bottom at smaller tube diameters. The experimental results of Othmer [18] with a tube diameter of 2 in. suggest that the effect is one of increased total film thickness since his results generally show lower heat transfer coefficients than those predicted by Nusselt's equation. The results of the present experiment show that at even smaller diameters the ratio of the measured to calculated heat transfer coefficients starts increasing with decreasing tube diameter. This is an opposite trend from that at larger tube diameters.

The two distinct patterns of deviation from Nusselt's solution can be seen more clearly by examining the ratio of the surface tension forces to the gravity forces on the condensate film. Consider any axial location along the tube and assume a slight inclination of the tube such that droplets are moving past the test location. Under

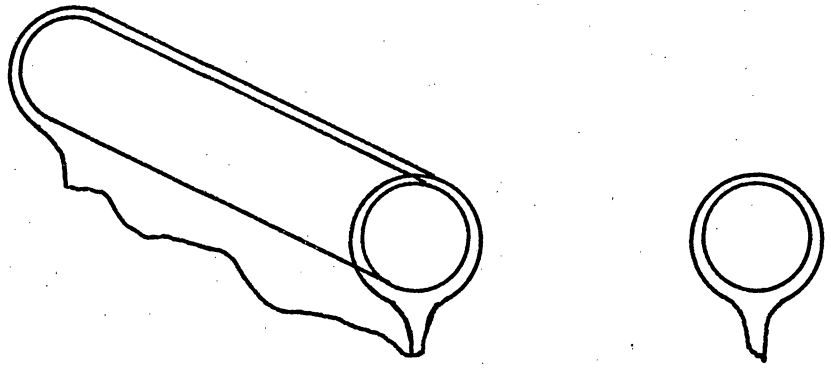

(a) Assumed Flow Pattern in the Analytical Solutions.

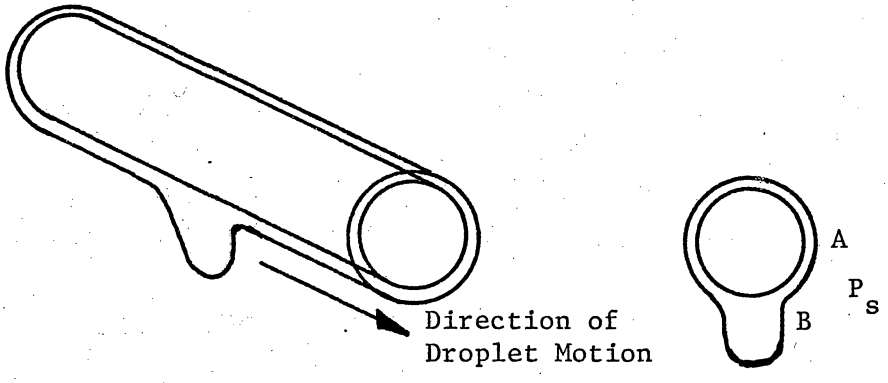


(b) Actual Flow Pattern on Small Diameter Tubes.

Figure 26. Comparison of Assumed Flow Pattern with Actual Flow Pattern on Small Diameter Tubes.

such a flow situation the condensate film at the test location experiences an impulse each time a droplet appears at the location. For simplicity, assume further that the cumulative effect of this flow situation is proportional to the effect of an imaginary flow pattern in which a drop site exists continually at all possible test locations. Considering Figure 26b under these assumptions, the pressure difference between the film and steam resulting only from surface tension is given by

$$P_A - P_s = 2\sigma/r_A \qquad \text{at} \qquad A$$

$$P_B - P_s = 2\sigma/r_B \qquad \text{at} \qquad B$$

but $r_A \simeq D_o/2$ and $r_B \simeq \infty$, therefore

$$P_A - P_s = 4\sigma/D_o$$

$$P_B - P_s = 0$$

This gives

$$P_A - P_B = 4\sigma/D_o$$

Two such pressures exists at a drop site. The net pressure as a result of surface tension is

$$\Delta P = 8\sigma/D_o$$

The force on the condensate film as a result of surface tension becomes

$$F = [\Delta P]\delta$$

$$= 8\sigma\delta/D_o$$

The gravity force on the film is equal to the weight of the film

$$W = \rho g[\pi D_o]\delta$$

The ratio is a dimensionless group, $N_d$

$$N_d = 8\sigma/[\pi\rho g D_o^2]$$

The results of the present experiment versus this dimensionless group are plotted in Figure 27. The solid line is an approximate curve fit for the experimental data. The broken line represents the expected trend at smaller values of the dimensionless number. The experimental data presented in the literature all fall in the range of $N_d$ smaller than 0.1. These latter data were not included in Figure 27 because of the large scatter in these data for reasons other than the surface tension effects. The broken line is a possible extrapolation taking for granted that the two-dimensional solutions represent the problem at negligible surface tension. This line is drawn to project the expected trend for $N_d$ near zero. The broken line is included merely for completeness and has not been verified as a satisfactory prediction for the heat transfer coefficients.

The two distinct patterns of deviation from Nusselt's equation are seen in Figure 27. For small values of $N_d$, the drop formation on the tube bottom results in a larger film thickness than that predicted by Nusselt's equation. This should be expected since the pressure force induced by surface tension is small in comparison with the gravity force on the film. Therefore the existence of drops can only add to the thickness of the film. As $N_d$ increases, the pressure force attributed to surface tension is comparable with the gravity force. These two forces act in the same direction against the viscous forces. The result is a thinner film than the analytically expected results. The curve starts increasing with increasing values of $N_d$.

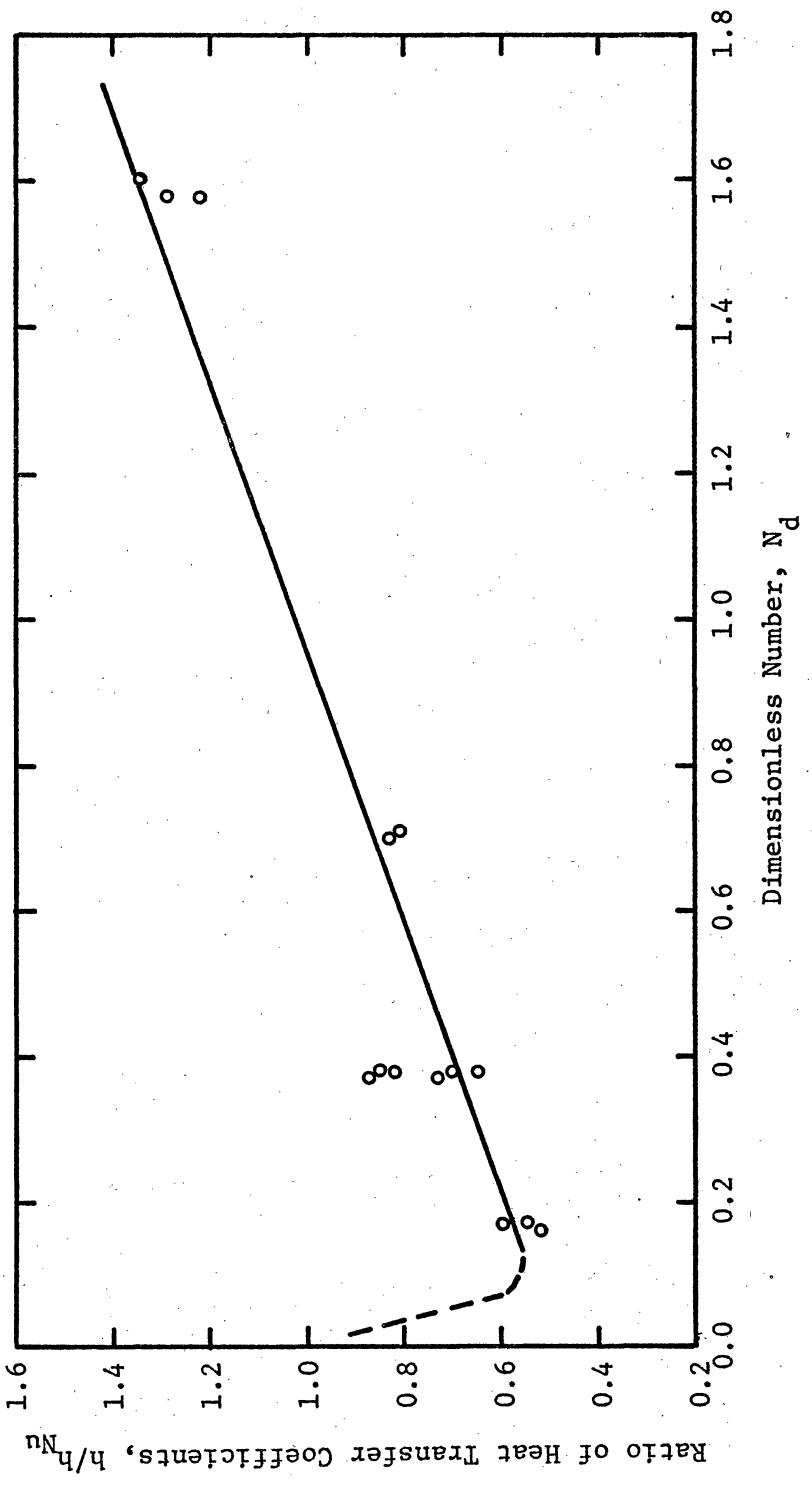


Figure 27. Ratio of Heat Transfer Coefficients versus Dimensionless Number.

# IV. CONCLUSIONS AND RECOMMENDATIONS

The heat transfer rates in condensation of pure vapors are affected by scale deposits, the condensation type, and the physical conditions of the specific problem. The effect of surface tension on the heat transfer on horizontal tubes becomes important for small tube diameters. The presence of droplets at the bottom of a small diameter tube under film condensation of a vapor results in significant deviations from the two-dimensional analytical predictions of the heat transfer coefficient. When the pressure force resulting from surface tension is small compared with the gravity force, the presence of droplets result in decreased heat transfer rates as compared with those prediced by the two-dimensional analytical solutions. When the pressure force induced by surface tension is comparable with the gravity force, a second effect is present and results in an increased heat transfer rate. The results of the present experimental study presented graphically in Figure 27 can be used for predicting heat transfer in film condensation of steam on horizontal tubes with diameters in the range of 1/8 in. to 3/8 inches. A similar behavior would be expected for condensing other vapors. Since the complete description of the problem is more involved than the simplified one presented in this study, a general correlation of the results was not attempted.

Contaminants in the vapor may change the texture of the condensing surface and result in a change in the condensation pattern. The more frequent condensation mode in practical applications is mixed

condensation. Prediction of heat transfer in such cases is complicated by two additional factors. The analytical prediction of mixed condensation is more complicated. Secondly, since a continuum of mixed condensation modes exist ranging from complete film to complete dropwise condensation, a knowledge of the possible condensation pattern is necessary for specific vapor-impurity combinations. Prediction of condensation heat transfer in practical applications therefore requires further research in surface chemistry as well as in the fluid dynamics of mixed condensation.

The following recommendations are noted as guidelines for further experimental studies of condensation heat transfer:

1. A complete understanding of the dynamics of film condensation under surface tension and gravity forces requires further theoretical and experimental studies. Experiments to determine film thicknesses and velocity profiles are recommended. It is desirable to directly measure the tube surface temperature at the condensing surface and to measure local heat transfer coefficients under well defined boundary conditions rather than overall heat transfer coefficients. It is important to note that there is a significant peripheral temperature variation in cases of large tube diameters expecially when the tube thermal conductivity is low.
2. Visual observation of the condensation type is necessary in condensation heat transfer measurements. The measurements can be used to support corresponding analytical predictions only if the condensation mode is known.

3. Wilson's method for calculating individual heat transfer coefficients from the overall coefficient cannot be used when the condensation pattern is changing. The constant condensate film coefficient assumption does not hold in such instances and erroneous results may be obtained.
4. In heat transfer measurements under mixed condensation patterns, the chemical composition of the vapor should be considered and the effect of composition on the type of condensation should be identified.

## LITERATURE CITED


1. Chao, B. T., Ed., Advanced Heat Transfer, University of Illinois Press, Urbana, Illinois, 1969, pp. 223-262.

2. Gröber, H., S. Erk and U. Grigull, Fundamentals of Heat Transfer, McGraw-Hill Book Company, Inc., New York, 1965.

3. Orrok, G. A., "The Transmission of Heat in Surface Condensation," Transactions of the ASME, Vol. 32, 1910, pp. 1139-1190.

4. McAdams, W. H., Heat Transmission, 3rd Ed., McGraw-Hill Book Company, Inc., New York, 1954, pp. 338-367.

5. Jakob, M., Heat Transfer, Vol. 1, John Wiley & Sons, Inc., New York, 1967, pp. 658-696.

6. Hampson, H., "The Condensation of Steam on a Metal Surface," Proceedings, General Discussion on Heat Transfer, Institution of Mechanical Engineers, 1951, pp. 58-61.

7. Hampson, H., "Heat Transfer during Condensation of Steam," Engineering, Vol. 172, 1951, pp. 221-223.

8. Boelter, L. M. K., V. H. Cherry, H. A. Johnson and R. C. Martinelli, Heat Transfer Notes, McGraw-Hill Book Company, Inc., New York, 1965, pp. 563-567.

9. Peck, R. E., and W. A. Reddie, "Heat Transfer Coefficients for Vapors Condensing on Horizontal Tubes," Industrial and Engineering Chemistry, Vol. 43, Part 4, 1951, pp. 2926-2931.

10. Henderson, C. L., and J. M. Marchello, "Role of Surface Tension and Tube Diameter in Film Condensation on Horizontal Tubes," AIChE Journal, Vol. 13, No. 3, 1967, pp. 613-614.

11. McAdams, W. H., and T. H. Frost, "Heat Transfer," Industrial and Engineering Chemistry, Vol. 14, 1922, pp. 13-18.

12. Othmer, D. F., "The Condensation of Steam," Industrial and Engineering Chemistry, Vol. 21, 1929, pp. 576-583.

13. Kirkbride, C. G., "Heat Transmission by Condensing Pure and Mixed Substances on Horizontal Tubes," Industrial and Engineering Chemistry, Vol. 25, 1933, pp. 1324-1330.

14. Wallace, J. L., and A. W. Davidson, "Condensation of Mixed Vapors," Industrial and Engineering Chemistry, Vol. 30, 1938, pp. 948-953.

15. Baker, E. M., and A. C. Mueller, "Heat Transfer Coefficients for the Condensation of Mixed Vapors of Immiscible Liquids," Industrial and Engineering Chemistry, Vol. 29, 1937, pp. 1067-1072.

16. Henderson, C. L., "Heat Transfer During Vapor Condensation in the Presence of Noncondensible Gas," Ph.D. Thesis, University of Maryland, 1967.

17. Othmer, D. F., and R. E. White, "Condensation of Vapors-Apparatus and Film Coefficients for Lower Alcohols," Transactions of the AIChE, Vol. 37, 1941, pp. 135-156.

18. Othmer, D. F., and S. Berman, "Condensation of Vapors," Industrial and Engineering Chemistry, Vol. 35, 1943, pp. 1068-1077.

19. Chen, M. M., "An Analytical Study of Laminar Film Condensation, Parts 1 and 2," Journal of Heat Transfer, Vol. 83, 1961, pp. 48-60.

20. Wilson, E. E., "A Basis for Rational Design of Heat Transfer Apparatus," Transactions of the ASME, Vol. 37, 1915, pp. 47-82.

21. Gebhart, B., Heat Transfer, 2nd Ed., McGraw-Hill Book Company, Inc., New York, 1971, pp. 430-456.

22. Dhir, V., and J. Lienhard, "Laminar Film Condensation on Plane and Axisymmetric Bodies in Nonuniform Gravity," Journal of Heat Transfer, Vol. 93, 1971, pp. 97-100.

23. Benedict, R. P., Fundamentals of Temperature, Pressure, and Flow Measurements, John Wiley & Sons, Inc., New York, 1969, pp. 65-98.

24. Kays, W. M., Convective Heat and Mass Transfer, McGraw-Hill Book Company, Inc., New York, 1966, pp. 150-202.

25. Kays, W. M., and E. Y. Leung, "Heat Transfer in Annular Passages--Hydrodynamically Developed Turbulent Flow with Arbitrary Prescribed Heat Flux," International Journal of Heat and Mass Transfer, Vol. 6, 1963, pp. 537-557.

26. Nagle, W. M., and T. B. Drew, "The Dropwise Condensation of Steam," Transactions of the AIChE, Vol. 30, 1933-34, pp. 217-255.

# APPENDIX I

## WILSON'S METHOD

Wilson [20] deduced a graphical representation of the heat transfer results which can be used to determine the individual heat transfer coefficients from the overall heat transfer coefficient. The following is an outline of a procedure similar to that of Wilson's.

The equation relating the overall thermal resistance to a series of thermal resistances is

$$R_t = R_o + R_w + R_i$$

where

$$R_t = 1/UA$$

$$R_o = 1/h_o A_o$$

$$R_w = \ell n\,[D_o/D_i]/[2\pi k_w L]$$

$$R_i = 1/h_i A_i$$

It is known that $h_i$ is sensitive to changes in the velocity, i.e.,

$$h_i \sim V^{0.83}$$

If it is assumed that $(R_o + R_w)$ is constant, the equation relating the resistances can be written as

$$R_t = a + bX$$

where

$$a = R_o + R_w$$

$$X = 1/V^{0.83}$$

If the total thermal resistances are measured at corresponding cooling water velocities, the values can be fitted into a linear relationship from which a and b are determined. The individual heat transfer coefficients can then be calculated using the equations of this section. The calculation procedure is given under Data Reduction Procedure in section II of the text.

# APPENDIX II

## CALIBRATION OF EQUIPMENT

The arrangement for the calibration of the thermocouples is shown in Figure 28. The mixing chamber thermocouples were calibrated for three points over the range 25 deg C to 75 deg C. A second degree polynomial curve was fitted through these points. Table II gives the calibration curves in functional form for the 4 mixing chamber thermocouples used in this experiment. Table III identifies the thermocouples used in each of the experimental runs.

The calibration curve for the rotameter is given in Figure 29. The calibration curve for the pressure gage is given in Figure 30.

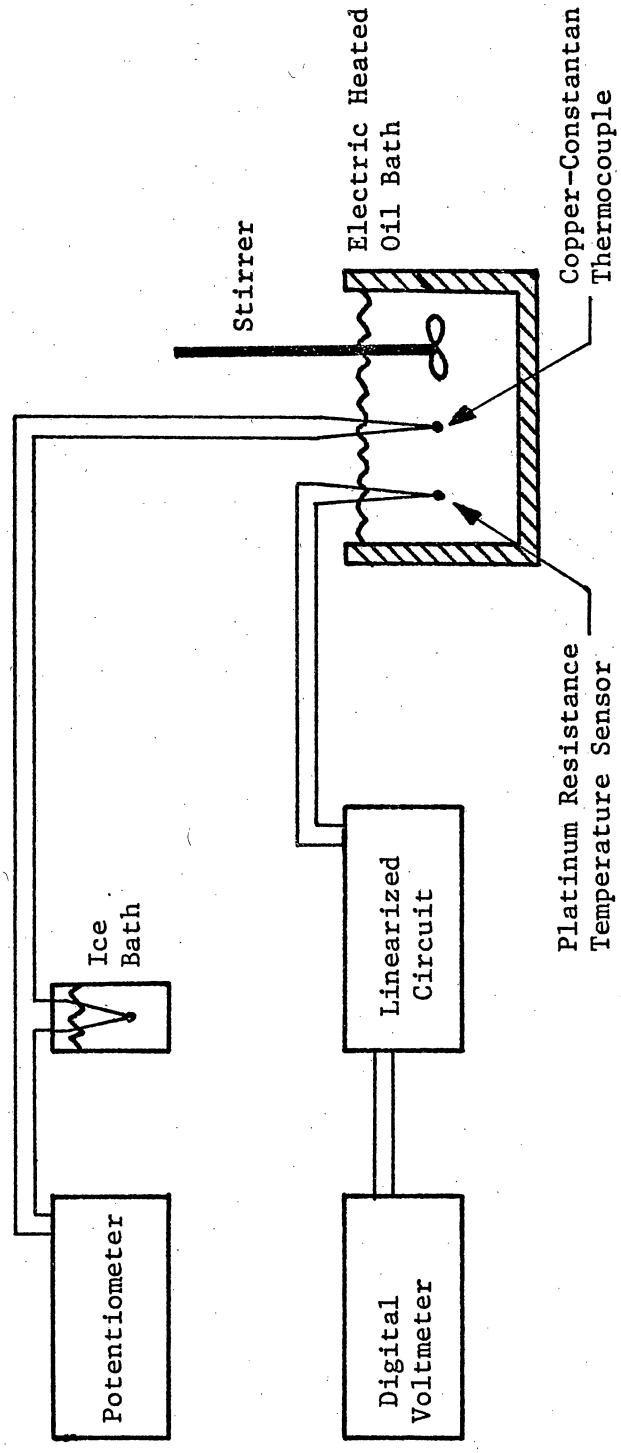


Figure 28. Arrangement for Calibration of the Thermocouples.

TABLE II. Calibration Table of Thermocouples

$$(\text{deg C}) = C_1(\text{mv})^2 + C_2(\text{mv}) + C_3$$

| Thermocouple No. | 1 | 2 | 3 | 4 |
|---|---|---|---|---|
| Thermocouple reading (mv) | 0.977 | 1.001 | 1.010 | 1.012 |
| Sensor reading (deg C) | 26.2 | 26.3 | 26.3 | 26.3 |
| Thermocouple reading (mv) | 2.002 | 1.934 | 2.013 | 2.018 |
| Sensor reading (deg C) | 49.8 | 49.8 | 49.8 | 50.0 |
| Thermocouple reading (mv) | 3.027 | 2.959 | 3.020 | 3.016 |
| Sensor reading (deg C) | 73.1 | 73.0 | 73.0 | 72.9 |
| $C_1$ | -0.14296 | -1.3057 | -0.30618 | -0.21960 |
| $C_2$ | 23.480 | 29.052 | 24.517 | 24.174 |
| $C_3$ | 3.430 | -1.4391 | 1.8365 | 2.0924 |

TABLE III. Thermocouples Used at Inlet and Exit Mixing Chambers for Different Experimental Runs

| Run No. | Inlet Mixing Chamber Thermocouple No. | Exit Mixing Chamber Thermocouple No. |
|---|---|---|
| 1 | 1 | 2 |
| 2 | 1 | 2 |
| 3 | 2 | 4 |
| 4 | 1 | 3 |
| 5 | 1 | 3 |
| 6 | 2 | 4 |
| 7 | 2 | 4 |
| 8 | 1 | 4 |
| 9 | 1 | 4 |
| 10 | 1 | 4 |
| 11 | 1 | 4 |
| 12 | 1 | 2 |
| 13 | 1 | 2 |
| 14 | 1 | 2 |

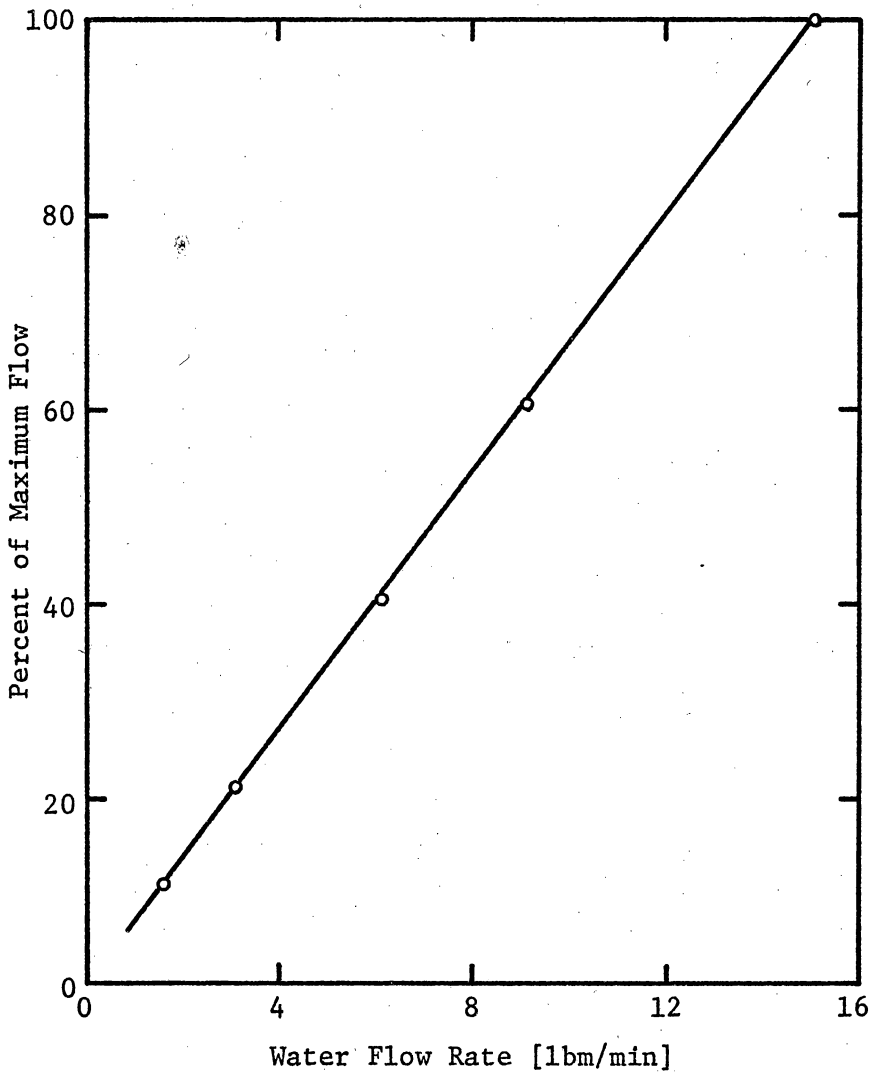


Figure 29. Rotameter Calibration.

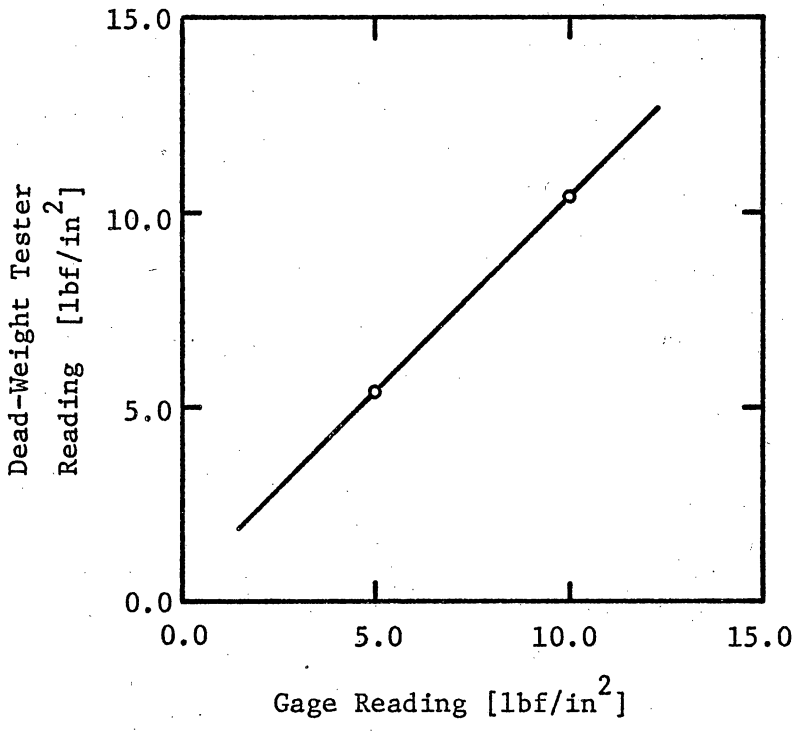


Figure 30. Bourdon Gage Calibration.

## APPENDIX III

## PHYSICAL PROPERTIES

Copper tube thermal conductivity, water specific heat capacity, and water density were taken as constants. Other properties of water were calculated from functional relationships given below.[1]

Thermal conductivity, Btu/hr-ft-deg F

$$k(T) = 0.2876 + 0.1007 \times 10^{-2}T - 0.2788 \times 10^{-5}T^2 + 0.1954 \times 10^{-8}T^3$$

where T is in deg F

Viscosity, lbm/ft-hr

$$\mu(TC) = 242.2/[2.1482[TC-8.435 + [8078.4 + [TC - 8.435]^2]^{1/2} - 120.0]$$

where TC is in deg C.

Surface tension, lbf/ft

$$\sigma(TC) = [-2.583333 \times 10^{-4}[TC]^2 - 0.1411666[TC] + 76.6] [30.48]^2 [7.376 \times 10^{-8}]$$

Latent heat of vaporization, Btu/lbm

$$\lambda(T) = 1073.73 - 0.45221T - 0.000163996T^2$$

---

[1]The functional relationships are taken from reference 16.

## APPENDIX IV

### DATA AND CALCULATED PARAMETERS

The data and calculated parameters of 14 experimental runs are presented in the following pages. Below is a key for the symbols used in the computer output:

| | | | |
|---|---|---|---|
| M = $m$ | [lbm/min] | TSA = $T_{s,a}$ | [deg F] |
| T1 = $T_1$ | [deg F] | TWOA = $T_{w,o,a}$ | [deg F] |
| T2 = $T_2$ | [deg F] | RO = $R_o$ | [deg F-hr/Btu] |
| TS = $T_s$ | [deg F] | QW = $q''_w$ | [Btu/hr-ft$^2$] |
| PS = $P_s$ | [lbf/in.$^2$] | NUFM = $Nu_{f,m}$ | [dimensionless] |
| TWI = $T_{w,i}$ | [deg F] | NUFC = $Nu_{f,c}$ | [dimensionless] |
| TWO = $T_{w,o}$ | [deg F] | PRF = $Pr_f$ | [dimensionless] |
| RE2 = $Re_2$ | [dimensionless] | NOH = $N_{Oh}$ | [dimensionless] |
| PR2 = $Pr_2$ | [dimensionless] | ND = $N_d$ | [dimensionless] |
| NUIC = $Nu_{i,c}$ | [dimensionless] | XI = $\xi$ | [dimensionless] |
| NUIM = $Nu_{i,m}$ | [dimensionless] | ZETA = $\zeta$ | [dimensionless] |
| | | H/HNU = $h/h_{Nu}$ | [dimensionless] |

DATA AND CALCULATED PARAMETERS
RUN NO. 1 TEST SECTION NO. 1

1. DATA

| | | | | | |
|---|---|---|---|---|---|
| M | 6.1 | 4.6 | 2.8 | 1.4 | 0.8 |
| T1 | 93.9 | 94.6 | 95.5 | 105.3 | 109.9 |
| T2 | 116.3 | 122.9 | 130.1 | 154.4 | 168.0 |
| TS | 219. | 220. | 219. | 225. | 221. |
| PS | 17.9 | 17.9 | 17.9 | 19.4 | 18.4 |

2. CALCULATED INTERNAL FLOW PARAMETERS

| | | | | | |
|---|---|---|---|---|---|
| TWI | 132. | 137. | 157. | 181. | 193. |
| TWO | 136. | 141. | 160. | 183. | 194. |
| RE2 | 56711. | 45496. | 29666. | 18039. | 10851. |
| PR2 | 3.8 | 3.5 | 3.3 | 2.6 | 2.4 |
| NUIC | 266. | 214. | 145. | 86. | 53. |
| NUIM | 306. | 241. | 159. | 88. | 52. |

3. CALCULATED CONDENSATE FILM PARAMETERS

| | | | |
|---|---|---|---|
| TSA | 221. | PRF | 2.0 |
| TWOA | 163. | NOH | 0.00075 |
| RO | 0.0102 | ND | 1.60 |
| QW | 214092. | XI | 0.030 |
| NUFM | 96. | ZETA | 0.060 |
| NUFC | 71. | H/HNU | 1.34 |

DATA AND CALCULATED PARAMETERS
RUN NO. 2 TEST SECTION NO. 1

1. DATA

| | | | | | |
|---|---|---|---|---|---|
| M | 4.5 | 4.0 | 3.5 | 3.0 | 1.7 |
| T1 | 88.1 | 84.8 | 87.7 | 85.2 | 91.9 |
| T2 | 116.4 | 115.9 | 120.3 | 122.9 | 142.6 |
| TS | 226. | 227. | 225. | 225. | 230. |
| PS | 20.4 | 20.4 | 19.9 | 19.4 | 21.7 |

2. CALCULATED INTERNAL FLOW PARAMETERS

| | | | | | |
|---|---|---|---|---|---|
| TWI | 134. | 137. | 143. | 144. | 169. |
| TWO | 138. | 141. | 146. | 147. | 171. |
| RE2 | 42357. | 37117. | 34002. | 29430. | 19626. |
| PR2 | 3.8 | 3.8 | 3.6 | 3.5 | 2.9 |
| NUIC | 209. | 188. | 171. | 149. | 97. |
| NUIM | 247. | 223. | 199. | 173. | 106. |

3. CALCULATED CONDENSATE FILM PARAMETERS

| | | | |
|---|---|---|---|
| TSA | 226. | PRF | 2.0 |
| TWOA | 149. | NOH | 0.00078 |
| RO | 0.0115 | ND | 1.58 |
| QW | 254036. | XI | 0.040 |
| NUFM | 85. | ZETA | 0.081 |
| NUFC | 66. | H/HNU | 1.29 |

DATA AND CALCULATED PARAMETERS
RUN NO. 3 TEST SECTION NO. 1

1. DATA

| | | | | | |
|---|---|---|---|---|---|
| M | 4.2 | 3.6 | 3.0 | 2.3 | 1.7 |
| T1 | 81.3 | 82.7 | 85.0 | 89.2 | 94.3 |
| T2 | 113.0 | 118.0 | 124.7 | 134.7 | 150.4 |
| TS | 226. | 226. | 227. | 228. | 231. |
| PS | 20.9 | 20.9 | 20.6 | 21.4 | 22.7 |

2. CALCULATED INTERNAL FLOW PARAMETERS

| | | | | | |
|---|---|---|---|---|---|
| TWI | 120. | 125. | 132. | 144. | 158. |
| TWO | 124. | 128. | 136. | 147. | 161. |
| RE2 | 38243. | 34423. | 30542. | 25873. | 20907. |
| PR2 | 3.9 | 3.7 | 3.5 | 3.1 | 2.7 |
| NUIC | 196. | 174. | 152. | 126. | 99. |
| NUIM | 381. | 334. | 285. | 229. | 170. |

3. CALCULATED CONDENSATE FILM PARAMETERS

| | | | |
|---|---|---|---|
| TSA | 228. | PRF | 2.1 |
| TWOA | 139. | NOH | 0.00080 |
| RO | 0.0127 | ND | 1.58 |
| QW | 262745. | XI | 0.044 |
| NUFM | 77. | ZETA | 0.092 |
| NUFC | 63. | H/HNU | 1.22 |

DATA AND CALCULATED PARAMETERS
RUN NO. 4 TEST SECTION NO. 2

1. DATA

| | | | | | |
|---|---|---|---|---|---|
| M | 13.2 | 11.5 | 10.3 | 8.6 | 7.3 |
| T1 | 63.4 | 63.4 | 63.4 | 63.4 | 64.3 |
| T2 | 82.3 | 84.4 | 86.1 | 89.1 | 93.4 |
| TS | 234. | 234. | 234. | 234. | 234. |
| PS | 23.9 | 23.9 | 23.9 | 23.9 | 23.9 |

2. CALCULATED INTERNAL FLOW PARAMETERS

| | | | | | |
|---|---|---|---|---|---|
| TWI | 106. | 109. | 114. | 119. | 125. |
| TWO | 110. | 113. | 117. | 123. | 128. |
| RE2 | 54128. | 48511. | 44290. | 38436. | 33968. |
| PR2 | 5.7 | 5.6 | 5.5 | 5.2 | 5.0 |
| NUIC | 315. | 284. | 260. | 227. | 199. |
| NUIM | 276. | 246. | 224. | 193. | 167. |

3. CALCULATED CONDENSATE FILM PARAMETERS

| | | | |
|---|---|---|---|
| TSA | 234. | PRF | 2.2 |
| TWOA | 118. | NOH | 0.00069 |
| RO | 0.0084 | ND | 0.70 |
| QW | 194081. | XI | 0.055 |
| NUFM | 65. | ZETA | 0.121 |
| NUFC | 79. | H/HNU | 0.83 |

DATA AND CALCULATED PARAMETERS
RUN NO. 5 TEST SECTION NO. 2

1. DATA

| | | | | | |
|---|---|---|---|---|---|
| M | 12.7 | 11.5 | 10.0 | 9.1 | 8.0 |
| T1 | 65.1 | 65.3 | 65.5 | 66.0 | 66.0 |
| T2 | 84.0 | 85.7 | 88.7 | 90.4 | 92.9 |
| TS | 230. | 230. | 231. | 231. | 231. |
| PS | 22.2 | 22.2 | 22.4 | 22.4 | 22.4 |

2. CALCULATED INTERNAL FLOW PARAMETERS

| | | | | | |
|---|---|---|---|---|---|
| TWI | 102. | 105. | 108. | 113. | 116. |
| TWO | 106. | 109. | 111. | 116. | 119. |
| RE2 | 53345. | 49252. | 44287. | 41056. | 37328. |
| PR2 | 5.6 | 5.5 | 5.3 | 5.2 | 5.0 |
| NUIC | 308. | 285. | 256. | 238. | 216. |
| NUIM | 322. | 296. | 262. | 242. | 218. |

3. CALCULATED CONDENSATE FILM PARAMETERS

| | | | |
|---|---|---|---|
| TSA | 231. | PRF | 2.3 |
| TWOA | 112. | NDH | 0.00071 |
| RO | 0.0087 | ND | 0.71 |
| QW | 192069. | XI | 0.054 |
| NUFM | 63. | ZETA | 0.124 |
| NUFC | 78. | H/HNU | 0.81 |

DATA AND CALCULATED PARAMETERS
RUN NO. 6 TEST SECTION NO. 3

1. DATA

| | | | | | |
|---|---|---|---|---|---|
| M | 11.6 | 10.4 | 9.1 | 7.7 | 5.7 |
| T1 | 62.4 | 62.4 | 62.4 | 62.7 | 63.9 |
| T2 | 86.6 | 89.6 | 91.7 | 95.6 | 103.2 |
| TS | 225. | 230. | 230. | 231. | 231. |
| PS | 20.9 | 22.4 | 21.9 | 22.4 | 22.4 |

2. CALCULATED INTERNAL FLOW PARAMETERS

| | | | | | |
|---|---|---|---|---|---|
| TWI | 115. | 121. | 126. | 132. | 143. |
| TWO | 118. | 123. | 128. | 134. | 145. |
| RE2 | 30820. | 28388. | 25479. | 22606. | 18286. |
| PR2 | 5.4 | 5.2 | 5.1 | 4.8 | 4.4 |
| NUIC | 192. | 176. | 158. | 140. | 112. |
| NUIM | 254. | 230. | 205. | 179. | 139. |

3. CALCULATED CONDENSATE FILM PARAMETERS

| | | | |
|---|---|---|---|
| TSA | 229. | PRF | 2.2 |
| TWOA | 130. | NOH | 0.00057 |
| RO | 0.0063 | ND | 0.38 |
| QW | 160211. | XI | 0.048 |
| NUFM | 86. | ZETA | 0.103 |
| NUFC | 104. | H/HNU | 0.82 |

DATA AND CALCULATED PARAMETERS
RUN NO. 7 TEST SECTION NO. 3

1. DATA

| | | | | | |
|---|---|---|---|---|---|
| M | 11.6 | 10.6 | 9.2 | 8.1 | 7.0 |
| T1 | 61.9 | 61.9 | 62.4 | 62.4 | 62.9 |
| T2 | 86.6 | 88.8 | 92.2 | 94.3 | 98.1 |
| TS | 226. | 228. | 228. | 230. | 228. |
| PS | 20.7 | 21.7 | 21.2 | 22.0 | 21.2 |

2. CALCULATED INTERNAL FLOW PARAMETERS

| | | | | | |
|---|---|---|---|---|---|
| TWI | 117. | 120. | 125. | 132. | 135. |
| TWO | 119. | 123. | 127. | 134. | 137. |
| RE2 | 30820. | 28726. | 25815. | 23381. | 20967. |
| PR2 | 5.4 | 5.3 | 5.0 | 4.9 | 4.7 |
| NUIC | 192. | 178. | 160. | 145. | 129. |
| NUIM | 253. | 233. | 206. | 186. | 163. |

3. CALCULATED CONDENSATE FILM PARAMETERS

| | | | |
|---|---|---|---|
| TSA | 228. | PRF | 2.2 |
| TWOA | 128. | NOH | 0.00058 |
| RO | 0.0062 | ND | 0.38 |
| QW | 164770. | XI | 0.048 |
| NUFM | 88. | ZETA | 0.104 |
| NUFC | 104. | H/HNU | 0.85 |

DATA AND CALCULATED PARAMETERS
RUN NO. 8 TEST SECTION NO. 3

1. DATA

| | | | | | |
|---|---|---|---|---|---|
| M | 15.1 | 12.1 | 10.6 | 9.1 | 7.6 |
| T1 | 66.0 | 66.4 | 66.4 | 66.8 | 67.2 |
| T2 | 82.7 | 86.6 | 88.3 | 91.7 | 95.9 |
| TS | 229. | 230. | 230. | 228. | 228. |
| PS | 21.4 | 21.9 | 21.9 | 21.4 | 21.4 |

2. CALCULATED INTERNAL FLOW PARAMETERS

| | | | | | |
|---|---|---|---|---|---|
| TWI | 94. | 101. | 106. | 108. | 113. |
| TWO | 97. | 103. | 109. | 111. | 115. |
| RE2 | 38217. | 32002. | 28564. | 25456. | 22243. |
| PR2 | 5.7 | 5.4 | 5.3 | 5.1 | 4.8 |
| NUIC | 236. | 198. | 178. | 158. | 138. |
| NUIM | 439. | 364. | 325. | 285. | 244. |

3. CALCULATED CONDENSATE FILM PARAMETERS

| | | | |
|---|---|---|---|
| TSA | 229. | PRF | 2.4 |
| TWOA | 107. | NDH | 0.00062 |
| RO | 0.0087 | ND | 0.38 |
| QW | 143364. | XI | 0.054 |
| NUFM | 63. | ZETA | 0.127 |
| NUFC | 97. | H/HNU | 0.65 |

DATA AND CALCULATED PARAMETERS
RUN NO. 9 TEST SECTION NO. 3

1. DATA

| | | | | | |
|---|---|---|---|---|---|
| M | 15.1 | 12.1 | 9.1 | 7.6 | 6.0 |
| T1 | 66.8 | 66.8 | 67.2 | 67.2 | 67.6 |
| T2 | 84.4 | 88.3 | 93.4 | 98.0 | 102.7 |
| TS | 228. | 228. | 228. | 229. | 230. |
| PS | 21.4 | 21.4 | 21.2 | 21.5 | 21.7 |

2. CALCULATED INTERNAL FLOW PARAMETERS

| | | | | | |
|---|---|---|---|---|---|
| TWI | 102. | 105. | 116. | 118. | 129. |
| TWO | 104. | 107. | 118. | 121. | 131. |
| RE2 | 39007. | 32644. | 25948. | 22763. | 19139. |
| PR2 | 5.6 | 5.3 | 5.0 | 4.7 | 4.4 |
| NUIC | 237. | 199. | 159. | 139. | 117. |
| NUIM | 399. | 331. | 259. | 222. | 184. |

3. CALCULATED CONDENSATE FILM PARAMETERS

| | | | |
|---|---|---|---|
| TSA | 229. | PRF | 2.3 |
| TWOA | 116. | NOH | 0.00060 |
| RO | 0.0078 | ND | 0.38 |
| QW | 147840. | XI | 0.051 |
| NUFM | 70. | ZETA | 0.117 |
| NUFC | 100. | H/HNU | 0.70 |

DATA AND CALCULATED PARAMETERS
RUN NO. 10 TEST SECTION NO. 3

1. DATA

| | | | | | |
|---|---|---|---|---|---|
| M | 15.1 | 12.1 | 9.1 | 7.6 | 6.0 |
| T1 | 68.1 | 68.5 | 69.3 | 70.1 | 70.6 |
| T2 | 86.6 | 90.4 | 96.3 | 101.4 | 105.2 |
| TS | 234. | 233. | 233. | 233. | 232. |
| PS | 23.3 | 23.2 | 23.1 | 23.2 | 22.4 |

2. CALCULATED INTERNAL FLOW PARAMETERS

| | | | | | |
|---|---|---|---|---|---|
| TWI | 107. | 113. | 122. | 126. | 137. |
| TWO | 110. | 116. | 125. | 128. | 139. |
| RE2 | 40003. | 33453. | 26816. | 23605. | 19651. |
| PR2 | 5.4 | 5.2 | 4.8 | 4.5 | 4.3 |
| NUIC | 238. | 200. | 161. | 140. | 118. |
| NUIM | 351. | 291. | 228. | 195. | 162. |

3. CALCULATED CONDENSATE FILM PARAMETERS

| | | | |
|---|---|---|---|
| TSA | 233. | PRF | 2.2 |
| TWOA | 124. | NOH | 0.00058 |
| RO | 0.0074 | ND | 0.37 |
| QW | 151219. | XI | 0.052 |
| NUFM | 74. | ZETA | 0.114 |
| NUFC | 102. | H/HNU | 0.73 |

DATA AND CALCULATED PARAMETERS
RUN NO. 11 TEST SECTION NO. 3

1. DATA

| | | | | | |
|---|---|---|---|---|---|
| M | 15.1 | 12.1 | 10.6 | 9.1 | 7.6 |
| T1 | 68.1 | 68.5 | 68.5 | 68.9 | 69.3 |
| T2 | 88.3 | 91.7 | 94.2 | 97.6 | 101.0 |
| TS | 233. | 233. | 232. | 233. | 235. |
| PS | 23.4 | 23.2 | 22.9 | 23.4 | 24.0 |

2. CALCULATED INTERNAL FLOW PARAMETERS

| | | | | | |
|---|---|---|---|---|---|
| TWI | 122. | 131. | 133. | 139. | 148. |
| TWO | 125. | 134. | 136. | 141. | 151. |
| RE2 | 40805. | 33942. | 30560. | 27191. | 23499. |
| PR2 | 5.3 | 5.1 | 4.9 | 4.7 | 4.5 |
| NUIC | 240. | 201. | 181. | 161. | 140. |
| NUIM | 252. | 209. | 187. | 164. | 140. |

3. CALCULATED CONDENSATE FILM PARAMETERS

| | | | |
|---|---|---|---|
| TSA | 233. | PRF | 2.1 |
| TWOA | 137. | NOH | 0.00055 |
| RO | 0.0059 | ND | 0.37 |
| QW | 166203. | XI | 0.048 |
| NUFM | 92. | ZETA | 0.100 |
| NUFC | 106. | H/HNU | 0.87 |

DATA AND CALCULATED PARAMETERS
RUN NO. 12 TEST SECTION NO. 4

1. DATA

| | | | | | |
|---|---|---|---|---|---|
| M | 15.1 | 13.5 | 12.0 | 10.6 | 9.1 |
| T1 | 63.9 | 64.3 | 64.3 | 64.3 | 64.3 |
| T2 | 80.8 | 82.2 | 84.6 | 86.0 | 88.8 |
| TS | 225. | 227. | 228. | 230. | 230. |
| PS | 20.0 | 20.9 | 20.7 | 21.4 | 21.4 |

2. CALCULATED INTERNAL FLOW PARAMETERS

| | | | | | |
|---|---|---|---|---|---|
| TWI | 114. | 122. | 123. | 130. | 134. |
| TWO | 116. | 123. | 124. | 132. | 135. |
| RE2 | 22394. | 20393. | 18635. | 16685. | 14778. |
| PR2 | 5.9 | 5.8 | 5.6 | 5.5 | 5.3 |
| NUIC | 153. | 140. | 128. | 116. | 103. |
| NUIM | 215. | 196. | 177. | 159. | 140. |

3. CALCULATED CONDENSATE FILM PARAMETERS

| | | | |
|---|---|---|---|
| TSA | 228. | PRF | 2.2 |
| TWOA | 126. | NOH | 0.00048 |
| RO | 0.0071 | ND | 0.17 |
| QW | 97374. | XI | 0.048 |
| NUFM | 77. | ZETA | 0.106 |
| NUFC | 140. | H/HNU | 0.55 |

DATA AND CALCULATED PARAMETERS
RUN NO. 13 TEST SECTION NO. 4

1. DATA

| | | | | | |
|---|---|---|---|---|---|
| M | 15.0 | 13.6 | 12.1 | 10.3 | 8.6 |
| T1 | 62.6 | 62.2 | 63.0 | 63.0 | 64.9 |
| T2 | 79.4 | 80.8 | 82.2 | 85.0 | 89.7 |
| TS | 222. | 226. | 223. | 231. | 232. |
| PS | 19.0 | 20.7 | 19.4 | 22.6 | 22.9 |

2. CALCULATED INTERNAL FLOW PARAMETERS

| | | | | | |
|---|---|---|---|---|---|
| TWI | 128. | 132. | 137. | 147. | 153. |
| TWO | 130. | 134. | 138. | 148. | 154. |
| RE2 | 21895. | 20155. | 18228. | 16029. | 14190. |
| PR2 | 6.0 | 5.9 | 5.8 | 5.5 | 5.2 |
| NUIC | 152. | 140. | 128. | 113. | 99. |
| NUIM | 163. | 150. | 136. | 118. | 102. |

3. CALCULATED CONDENSATE FILM PARAMETERS

| | | | |
|---|---|---|---|
| TSA | 227. | PRF | 2.1 |
| TWOA | 141. | NOH | 0.00045 |
| RO | 0.0061 | ND | 0.17 |
| QW | 96004. | XI | 0.043 |
| NUFM | 89. | ZETA | 0.089 |
| NUFC | 148. | H/HNU | 0.60 |

DATA AND CALCULATED PARAMETERS
RUN NO. 14 TEST SECTION NO. 4

1. DATA

| | | | | | |
|---|---|---|---|---|---|
| M | 15.1 | 13.6 | 12.1 | 10.6 | 9.1 |
| T1 | 63.9 | 63.9 | 64.1 | 64.3 | 66.0 |
| T2 | 81.7 | 83.1 | 85.0 | 86.4 | 91.8 |
| TS | 237. | 236. | 235. | 236. | 236. |
| PS | 24.1 | 24.1 | 24.1 | 24.1 | 24.1 |

2. CALCULATED INTERNAL FLOW PARAMETERS

| | | | | | |
|---|---|---|---|---|---|
| TWI | 110. | 113. | 116. | 126. | 126. |
| TWO | 112. | 114. | 118. | 127. | 127. |
| RE2 | 22655. | 20742. | 18858. | 16777. | 15297. |
| PR2 | 5.8 | 5.7 | 5.5 | 5.4 | 5.1 |
| NUIC | 154. | 141. | 129. | 116. | 104. |
| NUIM | 263. | 240. | 218. | 195. | 170. |

3. CALCULATED CONDENSATE FILM PARAMETERS

| | | | |
|---|---|---|---|
| TSA | 236. | PRF | 2.2 |
| TWOA | 120. | NOH | 0.00048 |
| RO | 0.0077 | ND | 0.16 |
| QW | 102364. | XI | 0.055 |
| NUFM | 71. | ZETA | 0.121 |
| NUFC | 136. | H/HNU | 0.52 |

The vita has been removed from the scanned document

# HEAT TRANSFER MEASUREMENTS IN FILM CONDENSATION OF STEAM ON SMALL DIAMETER HORIZONTAL TUBES

by

Mazhar Ünsal

(ABSTRACT)

Heat transfer coefficients were measured during film condensation of steam on horizontal tubes of 0.122, 0.182, 0.250, 0.375 inches in diameter. Scale effects were eliminated by repeated cleaning of the tubes. Filmwise, dropwise, mixed, and streaky condensation patterns of steam on the horizontal tubes were observed and photographed. The flow pattern in film condensation showed definite three-dimensional behaviour and was strongly affected by surface tension for the small tube diameters used. The measured heat transfer coefficients under film condensation showed differences as much as 50 percent from the two-dimensional analytical predictions.

A dimensionless number representing the ratio of the surface tension force to the gravity force was obtained from a physical analysis. The experimental results showed that when the surface tension force was small in comparison to the gravity force, the surface tension force acts to suppress the heat transfer. When the surface tension and gravity forces were of comparable magnitude, the heat transfer was augmented.